Different ways of evolving tool-using brains in teleosts and amniotes

Pierre Estienne, Matthieu Simion, Armin Jenett, Kei Yamamoto

Different ways of evolving tool-using brains in teleosts and amniotes

Pierre Estienne[1], Matthieu Simion[2], Arnim Jenett[2], Kei Yamamoto[1*]

[1]Paris-Saclay Institute of Neuroscience (NeuroPSI), Université Paris-Saclay, CNRS UMR9197, Saclay, 91400 France

[2]TEFOR Paris-Saclay, CNRS UMS2010, INRA UMS1451, Université Paris-Saclay, Saclay, 91400 France

*Correspondence: kei.yamamoto@cnrs.fr

SUMMARY

In mammals and birds, tool-using species are characterized by a high degree of encephalization with a relatively large telencephalon containing a higher proportion of total brain neurons compared to other species. Some teleost species in the wrasse family have convergently evolved tool-using abilities. In this study, we compared the brains of tool-using wrasses with various teleost species from a broad phylogenetic range. We show that in the tool-using wrasses, the telencephalon and the ventral part of the forebrain and midbrain are significantly enlarged compared to other teleost species, but do not contain a larger proportion of cells. Instead, this size difference is due to large fiber tracts connecting the dorsal part of the telencephalon (pallium) to the inferior lobe (IL), a ventral mesencephalic structure absent in amniotes. Such tracts were not present in other teleost species such as trout, zebrafish, or the *Astyanax* surface fish. The high degree of connectivity between the IL and the pallium in tool-using wrasses suggests that this unique teleostean structure contributes to higher-order cognitive functions. Considering how remarkably different their overall brain

organization is, we conclude that, unlike in amniotes, the evolution of non telencephalic structures might have been key in the emergence of higher-order cognitive functions in teleosts.

KEYWORDS

Encephalization, inferior lobe, pallium, neuroanatomy, teleosts, tool-users, wrasses

INTRODUCTION

In primates, the cerebral cortex is the center for higher-order cognition such as logical thinking or self-recognition. However, some birds, such as corvids and parrots, demonstrate comparable cognitive functions, even though they do not possess this six-layered cortical structure.[1,2] Remarkable behaviors indicative of so-called higher-order cognition include tool use[3–5] and mirror use,[6] which require causal reasoning, planning, or self-recognition.

Encephalization, the relative mass of the brain compared to body mass,[7] has long been used as a proxy for intelligence in vertebrates, with highly encephalized species being considered more intelligent.[8,9] Despite the high degree of encephalization in corvids and parrots, cognitive abilities in birds have long been underestimated due to their rather small brains compared to mammals. However, a more recent cell counting study has revealed that the brains of parrots and songbirds are extremely neuron-dense and contain on average twice as many neurons as primate brains of the same mass. Thus, some species of corvids and parrots have as many neurons in their pallium (the dorsal telencephalon that contains the cerebral cortex in mammals) as some species of primates.[10] This strongly suggests that mammals and birds have followed two independent trajectories of encephalization: an increase in cortical surface in mammals (with the cortex reaching a very large size in humans), and an increase in the neuronal density of the pallium in birds. Both trajectories led to an increase in the absolute number of telencephalic neurons in highly encephalized species of mammals and birds compared to poorly-encephalized ones. In other words, encephalization in amniotes (the clade containing mammals and birds) is mostly a process of "telencephalization".

Teleosts brains are generally much less encephalized compared to amniotes.[7] Nonetheless, some teleost fishes belonging to the family of wrasses (*Labridae*) exhibit tool use-like behavior[11] or mirror use behavior,[12] that are observed only in a few species of mammals and birds. Compared to amniotes, the organization of the teleost brain is much less known. Based on our previous studies, although similar behavioral phenotypes can be observed in amniotes and teleosts, the underlying brain anatomy is not conserved from their common ancestors. Many of the functional similarities are likely to be a consequence of convergent evolution.[13–16] Notably, teleosts possess a remarkable ventral structure called the inferior lobe (IL), which is absent in tetrapod brains and whose functions remain largely unknown.[13]

These observations raise the question of how encephalization occurred in the teleost lineage, and of how the brains of teleosts with remarkable cognitive abilities, such as wrasses, differ from other species. Is the teleost pallium the brain center that is responsible for higher-order cognitive functions similarly to the amniote brain? In order to uncover which brain structures are expanded in teleost species demonstrating complex behavioral repertoires, we examined the cellular composition of their major brain regions and compared them with other teleost species located at various phylogenetic positions. Wrasses had a larger telencephalon but, to our surprise, a similar relative number of telencephalic cells (i.e., the percentage of total brain cells present in the telencephalon) compared to other teleosts such as zebrafish.

Based on 3D reconstructions of fiber projections, we found that wrasses have major fiber tracts connecting the pallium and IL which constitute massive arborizations in both structures. This would contritube to the relatively larger telencephalon and IL found in wrasses, and may explain their cognitive abilities.

Altogether, our study illustrates how encephalization in teleosts and amniotes followed very different evolutionary paths allowing for the emergence of "tool-using brains".

RESULTS

The tool-using wrasse *Choerodon anchorago* has more cells in its brain than the hamster

The body mass and brain mass were measured for 11 species of teleost: a group of 3 wrasse species (*Choerodon anchorago*, *Labroides dimidiatus, Thalassoma hardwicke*), a group of 4 cichlid species (*Maylandia zebra*, *Neolamprologus brichardi*, *Ophthalmotilapia boops*, *Amatitlania nigrofasciata*), and a group of 4 other species (the medaka (*Oryzias latipes*), zebrafish (*Danio rerio*), *Astyanax* surface fish (*Astyanax mexicanus*), and trout (*Salmo trutta*), hereafter referred to as the “outgroup”) (Figure 1, see STAR Methods). Total number of cells in the brain was determined using the isotropic fractionator (STAR Methods).

Remarkably complex behaviors (tool use in the case of *C. anchorago* and *T. hardwicke,*[17,18] and social cognition in the case of *L. dimidiatus*[19–21]) have been reported in the group of wrasses. Cichlids are phylogenetically close to wrasses and display relatively complex social and cognitive behaviors, although no instances of tool use have been observed[22–25]. By contrast, no such behaviors have been reported in the “outgroup” species.

Among the wrasses studied, body mass ranged from 1.55 to 91.52 g, brain mass from 34.62 to 338.8 mg, and total number of cells in the brain from 45.7 to 185.08 million (Table 1). Wrasses were wild caught and generally tended to be young adults, however, one large adult of *C. anchorago*, weighing around ten times as much as the

other individuals, was also sampled. Statistical analysis showed that the data from this large individual did not impact the statistical significance of our results (Figures S1-7; see Document S1). In cichlids, body mass ranged from 5.15 to 20.28 g, brain mass from 42.43 to 96.94 mg and total number of cells in the brain from 37.54 to 61.78 million (Table 1). In the "outgroup", body mass ranged from 0.492 to 177.15 g, brain mass from 8.38 to 354.73 mg and total number of cells in the brain from 6.66 to 100.84 million (Table 1).

Compared to previously published data, teleosts have smaller brains than birds, primates or rodents of similar body mass (Figure 2A). By contrast, teleost brains contain more cells than the brains of rodents of similar body mass, albeit not as many as birds and primates, (Figure 2B). For instance, the brain of the tool-using wrasse *C. anchorago* contains on average more cells than the brain of the nearly 2 times heavier hamster (*Cricetus cricetus*).

Cellular density inside the teleost brain is higher than in birds and mammals, with teleosts having as many cells as rodent brains more than 4 times larger (Figure 2C). For example, the large *C. anchorago* individual sampled had 301.9 million cells in its brain, nearly as many cells as a rat (*Rattus norvegicus*), even though its brain is 2.6 times smaller.

Encephalization and relative mass or number of cells in the telencephalon of teleosts are not correlated

Residuals obtained by fitting a $\log^{10}$-$\log^{10}$ regression of brain mass against body mass data from this dataset with previously published data on actinopterygians (Figure 3) using a phylogenetic generalized least square (PGLS) model ranged from -0.142 (*D. rerio*) to 0.38 (the wrasse *T. hardwicke*), with only one other species (*C. anchorago*)

with a residual >0.30 (Figure 3, Table S1). Excluding the large *C. anchorago* from our analysis gave a residual of 0.488 for *C. anchorago*, placing it above *T. hardwicke* (Table S3, see Document S1). Overall, these two tool-using species were the most encephalized of our dataset.

In order to compare the degree of encephalization with the relative mass and cellular composition of major brain regions, the brains of ten species were dissected into five parts (Figure 4A): the telencephalon (Tel), the optic tectum (TeO), the rest of the Forebrain/Midbrain (rFM), the cerebellum (Cb) and the rest of the Hindbrain (rH) following the rostro-caudal and dorso-ventral axis (Figures 4B-E, STAR Methods). The structures were weighed and the number of cells contained in each structure was determined using the isotropic fractionator (STAR Methods). No statistically significant correlations were found between encephalization and the relative mass and relative number of cells of the Tel, TeO, rFM, Cb (Figures S8A-D). The only structure that showed a statistically significant correlation with encephalization was the rH (Figure S8E), with a negative correlation for both the relative mass and relative number of cells (STAR Methods). This indicates that more encephalized species of teleosts have a relatively smaller rH containing a relatively smaller number of cells.

These results suggest that teleost brains have evolved very differently from amniote brains. Unlike in mammals and birds, encephalization in teleosts is not synonymous with "telencephalization".

Wrasses have a relatively larger Tel and rFM than other teleosts, but not a larger relative number of cells than other teleosts

One to one species to species comparison didn’t reveal any consistent differences in either the relative mass or relative number of cells across structures (Figure S9, STAR

Methods). However, a trend towards larger Tel and rFM was observable when examining wrasses as a whole (Figure S9). Wrasses have large brains and display the most flexible behavioral repertoires, including tool use. We thus aimed to investigate what sets their brains apart morphologically from other teleosts. To this end, the relative mass and number of cells in the five major regions of the brains of all wrasse species were compared with those of the other species of teleosts sampled in this study (Figures 5 and 6).

The relative mass of the Tel and rFM was significantly higher in wrasses compared to other teleosts, with the Tel accounting for 24.11% ± 3.78% of total brain mass in wrasses compared to 15.43% ± 3.74% in other species (Figure 5A). While the Tel in wrasses is larger than in other teleosts, it remains modest when compared to amniotes. The rFM accounted for 28.82% ± 2.46% of total brain mass in wrasses compared to 24.72% ± 3.43% in other species (Figure 5C). The relative mass of the Cb and rest of the rH were significantly lower in wrasses compared to other teleosts (Figures 5D-E). No significant difference was found in the relative mass of the TeO between the two groups (Figure 5B).

Despite the larger size of the Tel and rFM in wrasses, isotropic fractionator data revealed that there is no significant difference in the relative number of cells in these two structures compared to other species. The Tel accounted for 12.02% ± 6.04% of total brain cells in wrasses compared to 8.49% ± 2.54% in other species (Figure 6A), while the rFM accounted for 12.04% ± 2.76% of total brain cells in wrasses and 12.39% ± 2.47% in other species (Figure 6C). No significant difference in relative number of cells was found in either the Cb (Figure 6D) or TeO (Figure 6B), whereas the rH (Figure 6E) accounted for a significantly smaller relative number of cells in wrasses compared to other species (2.18% ± 0.64% and 5.41% ± 1.64%, respectively).

Similar results were obtained when comparing the group formed by wrasses and cichlids together to the "outgroup" (Figures S10 and S11, STAR Methods).

Overall, these results show that wrasses have a relatively larger Tel and rFM compared to other teleosts. Surprisingly, however, these two structures do not contain a larger proportion of cells than in other teleosts.

Pallium and IL display increased connectivity in wrasses compared to other teleosts

We hypothesized that the increase in mass observed in the Tel and rFM of wrasses is due to an increase in the neuropil of these structures. To verify this hypothesis, we performed selective visualization of the fibers in the Tel and rFM. Whole brains of the wrasse *C. anchorago*, the cichlid *N. brichardi*, the trout *S. trutta*, the *Astyanax* surface fish *A. mexicanus*, and the zebrafish *D. rerio* were cleared, stained with DiI, and imaged on a light-sheet microscope (Figure 7, STAR Methods).

3D reconstruction of the DiI-stained fibers in the Tel and rFM of wrasses and cichlids revealed the presence of enriched fiber labeling in the Tel and rFM. Most of the IL, the ventral-most part of the rFM, was filled with fibers in wrasses (Figure 7A; in purple), while fiber labeling was sparse in the other species examined (trout, Figure 7C; *Astyanax* surface fish, Figure 7D; zebrafish, Figure 7E; in purple).

Wrasses (Figure 7A) and cichlids (Figure 7B) also possess a remarkable amount of fibers in an oval-shaped structure closely related to the IL called the corpus glomerulosum pars rotunda (GR),[26,27] which may also account for their relatively large rFM. Interestingly, this structure was not visible in *Astyanax* surface fish, zebrafish, nor trout (Figures 7A-E). GR is known to receive visual inputs from TeO and the pretectum

(PT), and to be reciprocally connected with the IL.[26–28] In addition, we found that GR is highly connected with the pallium in wrasses and cichlids (see below; Figures 7A-B).

The telencephalic fibers in the wrasse almost completely occupy the entire pallium. Those fibers converge onto two major tracts that we refer to as "pallio-lobar tracts" (see Discussion): the ventrally located tract, connecting the pallium and the ventral IL ipsilaterally (Pal-IL; Figure 7A; in green), and the dorsally located tract, connecting the pallium and IL through GR ipsilaterally (Pal-GR; Figure 7A; in magenta). The same tracts are also present in the cichlid brain, albeit more modestly, with a much smaller fiber arborization in both the pallium and IL (Figure 7B). A tract tracing study using the lipophilic dye NeuroVue (Figure S12, STAR Methods) confirmed these results, demonstrating the presence of a direct connectivity between the pallium and IL in the wrasse and cichlid brains. Strikingly, in trout, zebrafish, and *Astyanax* surface fish, these tracts were not detectable, and only minimal arborization was found in the pallium and the IL.

There are two fiber tracts observable in all species examined. One is made up of projections from the preglomerular nucleus (PG) to the pallium,[15,29] which are known to be sensory afferents (Figure 7; in orange). These are the major sensory afferents to the pallium of the trout, zebrafish, and *Astyanax* surface fish. In the wrasse, however, these sensory projections occupy a much smaller relative portion of the pallium (Figure 7A; in orange), as the pallio-lobar tracts are extremely developed. The tract from PG runs along with the Pal-IL tract and terminates in the lateral zone of the dorsal telencephalic area (Dl). The other tract present in all species is the one connecting the IL with the PT (Figure 7; in magenta). In the trout, zebrafish, and *Astyanax* surface fish, this is the major IL connectivity with the rostral aspect of the brain. In the wrasse, the

IL is also connected with PT, but this tract appears to be only a relatively small branch of the larger Pal-GR tract (Figure 7A; in magenta).

The presence of the pallio-lobar tracts is unrelated to absolute or relative brain size, as the large brained trout did not possess them. Thus, the main difference in brain organization between tool-using fishes and other species is the presence of a large quantity of fibers connecting the IL to the pallium in tool-using fishes, while the IL is merely connected with the PT in other species. Another intriguing observation was that there is no remarkable projections from the pallium to the subpallium (ventral part of the telencephalon, containing the striatum) in any of the species we examined, including the wrasse. This suggests that teleosts may not possess fiber tracts corresponding to the cortico-striatal projections of mammals.

Overall, the presence of the pallio-lobar tracts and their extreme enlargement in wrasses may thus explain the expansion of their Tel and rFM without a corresponding increase in the relative number of cells in those structures. This increase in the relative quantity of fibers in tool-using teleost species also parallels what has been observed in the mammalian telencephalon, where primates have a larger proportion of white matter compared to rodents.[30]

DISCUSSION

Encephalization is a process of telencephalization in amniotes, but not in teleosts

Mammals and birds have taken two different trajectories of encephalization that have converged onto a process of “telencephalization”, whereby the telencephalon (and in particular the pallium) becomes massively enlarged in highly encephalized species. Our study shows that the encephalization process happened differently in teleosts.

Sampling of a phylogenetically broad range of teleost species revealed that encephalization in teleosts leads to an enlargement of most of the examined brain regions, both in terms of mass and relative number of cells. That is, there was no single structure becoming particularly prominent in highly encephalized teleosts compared to less encephalized ones. Even in the tool-using species (*C. anchorago*), the telencephalon is of a modest size, representing only 27.8% of total brain mass. This is in stark contrast to amniotes, where the telencephalon makes up 80% of total brain mass in tool-using species of primates, parrots and corvids.[10,31]

Conversely, the remarkably large structure in teleosts is rFM. In previous amniote studies,[10,31] the brain structures corresponding to rFM, TeO and rH were pooled together and called “rest of brain” on account of their small relative size compared to the telencephalon and cerebellum. While this “rest of brain” represents merely 10 to 25% of total brain mass in primates, parrots and corvids,[10,31] it does represent 61.1% in the tool-using wrasse *C. anchorago*.

The modest telencephalon and large “rest of brain” of teleosts, even in relatively highly encephalized tool-using species, indicates that unlike in amniotes, encephalization in teleosts is not a process of telencephalization. Consequently, it appears that teleosts have evolved a different overall brain organization compared to amniotes.

Evolution of teleost-specific brain structures with no tetrapod homolog

The rFM corresponds to the ventral part of the forebrain and midbrain, while the Tel and TeO represent the dorsal parts of the forebrain and midbrain respectively. As the rFM is large in teleosts, accounting for a quarter to a third of total brain mass, it appears that teleost brains are a lot more “ventralized” compared to amniote brains. The rFM

of teleosts includes the IL, GR, and PG, structures that do not exist in tetrapods and which account for a large part of total brain mass in teleosts.

The IL in particular appeared to account for most of the rFM volume, and was especially enlarged in wrasses. The IL was long considered to be of hypothalamic origin, and used to be named “inferior lobe of the hypothalamus” as a result. A recent study[13] has demonstrated that the developmental origin of the IL is in fact mainly mesencephalic, while the cell populations surrounding the lateral recess of the hypothalamic ventricle, which represent a small part of the IL, are of hypothalamic origin. Bloch et al. (2019)[13] has suggested that in the species with a large IL, it is mainly this mesencephalic part that becomes enlarged, and not the hypothalamic part.

Another structure of the rFM that is mostly made up of cells of a mesencephalic origin is PG, which plays a role equivalent to the amniote thalamic nucleus as shown by our previous study.[15] In that sense, it appears that teleost brains are a lot more mesencephalized than amniote brains.

On top of the PG, GR is also considered to have important sensory (especially visual) functions, while having no homolog in tetrapod brains.[26–28] In fact, GR appears to be a specialized visual nucleus present only in some groups of teleosts which possess large connectivity between the pallium and IL. Thus, we consider GR a part of the IL complex.

Altogether, sensory systems in teleosts and tetrapods are not as conserved as previously thought, but have evolved independently in each lineage. Since pallial projections to the subpallium are not visible in teleosts, it is possible that the motor system, which relies on pallial projections to the striatum in amniotes,[32,33] is not conserved either. It may be that equivalent motor functions in teleosts rely on other brain structures.

Overall, teleosts display marked differences in the organization of their brains compared to amniotes, with mesencephalic structures accounting for a much larger proportion of total brain mass and playing a prominent role in sensory/motor processing.

Different ways of evolving tool-using brains

Our current study revealed that in the wrasse and cichlid brains, the IL is highly connected with the pallium. This seems to be especially true in tool-using species, which points to the involvement of both structures in this type of cognitive function.

As some previous studies already suggested[13,34], this challenges the previous notion that the IL is merely a food motivation center.[35–38] IL receives gustatory information [27,39–41], and due to its position just next to the hypothalamus, it was thought to be homologous to the lateral hypothalamus of mammals[38]. Direct electrical stimulation of the IL resulted in behaviors such as bitting at a mirror or snapping at objects in freely moving fish[35,36], and IL activation was found during detection of moving objects in larval zebrafish[37]. With the assumption that the IL was homologous to the mammalian hypothalamus, these functional data have been interpreted as the IL playing a role in feeding behaviors. However, since this previous view of IL homology has been shown to be erroneous[13], a reinterpretation of this data is necessary.

In addition to gustatory inputs, IL receives visual inputs from the TeO via the pretectum (PT)[26–28,37]. In the species where GR is present, it has been suggested that IL also receives auditory[26] and somatosensory[28] information. As a result, IL has also been proposed to be a multi-sensory integration center.[27,28,40,42] And since its main output is to the lateral valvular nucleus, which projects to the cerebellum,[27,43] its functions may be motor-related. This sensory input and motor output connectivity pattern in IL is rather similar to what has been found in the amniote pallium. Since the

teleost pallium itself receives sensory information from different modalities (e.g. auditory and visual inputs via PG), teleost brains seem to possess two separate sensory integration centers (Figure 8).

The presence of multimodal inputs to the IL is likely to be a common feature in teleosts, but the particularity of the wrasse and cichlid brains is the IL's intense connectivity with the pallium. The IL of other fish like trout, *Astyanax* surface fish, and zebrafish is mostly connected rostrally with PT, which is involved in stereotyped movements such as the optokinetic response[44,45] or the prey detection J-turn in larval zebrafish[46]. Those types of movements are sufficient for simple foraging behaviors without flexibility. It is then possible that the uniquely elaborated connectivity with the pallium present in wrasses and cichlids may have allowed for the emergence of their complex behavioral repertoire. The large gustatory inputs of the IL may for instance be involved in different functions than just eating in these species. As fish do not have hands, they use their mouth to manipulate objects, and likely have fine discriminative touch and motor control via the lips and oral cavity, functions which could involve the IL.

The presence of a higher-order association center in the teleost pallium has hardly been investigated so far. An interesting observation in this study was that the primary sensory areas in the tool-using wrasse are relatively small compared to other species. It is known that in mammalian and avian pallium, the primary sensory areas become relatively small in primates and corvids, with higher-order areas occupying a larger amount of the pallium.[47–49] This also seems to be the case in wrasses, and thus their enlarged pallium may be involved in higher-order processing allowing for tool use behaviors.

In conclusion, our findings revealed that the encephalization process in teleosts is different from what has previously been described in amniotes. While the pallium also appears to be important for higher-order cognitive functions in teleosts, the large pallio-lobar tracts in the tool-using fishes demonstrate the functional importance of the IL in relation to the pallium, which may be critical for such complex behaviors. Since the IL has no homolog in amniotes, at least three different brain organizations enabling higher-order cognitive functions may have evolved independently in mammals, birds and teleosts.

STAR METHODS

RESOURCE AVAILIBILITY

Lead contact

Further information and requests for resources and reagents should be directed to and will be fulfilled by the lead contact, Kei Yamamoto (kei.yamamoto@cnrs.fr).

Materials availability

This study did not generate new unique reagents.

Data and code availability

Data reported in this paper will be shared by the lead contact upon request.

This paper does not report original code.

EXPERIMENTAL MODEL AND SUBJECT DETAILS

Animals

11 species of teleost were examined: a group of 3 wrasse species (*Choerodon anchorago*, *Labroides dimidiatus, Thalassoma hardwicke*), for which complex

behaviors (tool use and social cognition) have been reported, 4 cichlid species (*Maylandia zebra*, *Neolamprologus brichardi*, *Ophthalmotilapia boops*, *Amatitlania nigrofasciata*), which are phylogenetically close to wrasses and are capable to a lesser extent of complex behaviors, and a group of 4 other species (the medaka (*Oryzias latipes*), zebrafish (*Danio rerio*), *Astyanax* surface fish (*Astyanax mexicanus*), and trout (*Salmo trutta*)) for which no such behavior has been observed.

Adult individuals of zebrafish (*Danio rerio*), medaka (*Oryzia latipes*) and *Astyanax mexicanus* were obtained from the animal facility in NeuroPSI (Saclay, France). Adult trouts (*Salmo trutta*) were sourced from the animal facility at INRAE (Jouy-en-Josas, France).

Sexually mature individuals of both sexes of wrasse and cichlid species were sourced from commercial providers (*Choerodon anchorago*, *Labroides dimidiatus*, *Thalassoma hardwicke*: Marine Life (Paris, France); *Maylandia zebra, Neolamprologus brichardi* and *Ophthalmotilapia boops*: Abysses (Boissy-Saint-Léger, France); *Amatitlania nigrofasciata*: Aquariofil.com (Nîmes, France)). Wrasses were wild caught and tended to be young adults, but one large adult of *Choerodon anchorago* weighing around ten times as much as the other individuals was also sampled. Statistical analysis showed that the data from this large individual did not impact the statistical significance of our results (see Document S1).

Brain sampling

Zebrafish and medaka specimens were euthanized in ice-cold water, weighed on a precision scale (PI-225DA, Denver Instrument) and fixed in ice-cold 4% paraformaldehyde (PFA; Electron Microscopy Science) in 0.01M phosphated buffer saline containing 0.1% Tween 20 (PBST; Fisher Scientific). 24 hours post-fixation,

brains were dissected, weighed on a precision scale and kept in 4% PFA in PBS for another 24 hours before being transferred in anti-freeze solution (30% glycerol, 30% ethylene glycol, 30% H_20, 10% PBS 10X) and kept at -20°C for later use.

Trout specimens and one individual of *Amatitlania nigrofasciata* were euthanized by an overdose of 0.4% tricaine methanesulfonate added to fish water (MS222; Sigma Aldrich), weighed on a scale (PI-2002, Denver Instrument) and decapitated. All other fish specimens were euthanized by an overdose of MS222, weighed, and immediately perfused transcardially with 4% PFA in PBS. Skulls were partly dissected to expose the brain and kept under agitation at 4°C in 4% PFA in PBS. 24 hours post-fixation, brains were dissected, weighed on a precision scale, and kept in 4% PFA in PBS for another 24 hours before being transferred in anti-freeze solution and kept at -20°C for later use. Brains used for NeuroVue tract-tracing were kept in 4% PFA at 4°C until use.

All procedures were conducted in compliance with the official regulatory standards of the French Government.

METHOD DETAILS

Dissection for isotropic fractionator

The medaka brains (n=5) were left undissected.

The brains of n=5 individuals of each species, except the trout (n=4), *M. zebra* (n=3), *C. anchorago* (n=4), *L. dimidiatus* (n=3), *T. hardwicke* (n=3) and *O. boops* (n=3) were rinsed in PBS and embedded in 3% agarose containing 1% Tween 20 and sectioned at 300 µm in the frontal plane with a vibratome (Leica VT 1200S). Under a stereomicroscope (Olympus SZX7), the brain was manually dissected using a

microsurgical knife (Stab Knife 5mm, 15 degrees; Surgical Specialties Corporation) into five regions following the rostro-caudal and dorso-ventral axis (Figure 4).

The dorsal part of the secondary prosencephalon, which includes the telencephalon and the dorso-rostral part of the optic recess region (ORR),[16,51] was excised. This region was labelled “telencephalon” (Tel). The second region dissected was the dorsal part of the mesencephalon, which includes the tectum opticum and the torus semicircularis and was labelled “optic tectum” (TeO). The third region included the ventral part of the secondary prosencephalon (i.e., the hypothalamus), the diencephalon and the ventral part of the mesencephalon (i.e., the tegmentum and the inferior lobe) and was labelled “rest of the forebrain/midbrain” (rFM). The fourth excised region was the dorsal part of the rhombencephalon (i.e., the cerebellum) (Cb). Finally, the fifth region excised was the ventral part of the rhombencephalon and was labelled “rest of the hindbrain” (rH).

Sections were dried with a Kimtech paper towel (Kimberly-Clark), weighed on a precision scale and kept in 4% PFA for later use. Due to overall shrinking of the whole brain in anti-freeze solution, these measures were only used to determine the relative mass of the different brain structures.

Isotropic fractionator

The number of cells in the five main regions of the teleost brain was determined using the isotropic fractionator method.[52] This method produces results similar to unbiased stereology.[53,54] Each structure was manually homogenized for 5 to 8 minutes in 100 µL 40 mM sodium citrate (Sigma Aldrich) with 1% Triton X-100 per 10 mg of tissue using a 0.5 mL or 2 mL Tenbroeck tissue grinder (Ningbo Ja-Hely Technology Co., Ningbo, China) depending on the weight of the structure.

Once an isotropic suspension of isolated cell nuclei was obtained, the suspension was pipetted and transferred to Eppendorf tubes for zebrafish brains or Falcon tubes for other species. Pestle and grinder were both washed with dissociation solution multiple times and rinses were pipetted into the tube containing the suspension. The suspension was then centrifuged at 4000g for 10 minutes, and the supernatant was collected into a separate tube. The cell nuclei in both the suspension pellet and the supernatant were stained by adding 1mL of PBS with 1% 4′,6-diamidino-2-phenylindole (DAPI; Sigma Aldrich). Additionally, a predetermined volume of PBS was added to the suspension to adjust the nuclei density for counting. Both the suspension and the supernatant were maintained homogenous by constant agitation.

To determine the total number of cells in the tissue, the nuclear density of both the suspension and the supernatant were determined. Four 10 µL aliquots of the suspension were counted under an epifluorescence microscope (Axio Imager, Zeiss) with X200 magnification using a Blaubrand Malassez counting chamber (Brand Gmbh, Wertheim, Germany). Variation between aliquots had to be <15%, otherwise one to four additional aliquots were counted to reach the threshold. Four aliquots of the supernatant were similarly counted to account for nuclei removed during pipetting. Mean nuclear density in the suspension and the supernatant was multiplied by their total volume and added up to determine the total number of cells in the brain tissue.

The supernatant was afterwards discarded, and the suspension was centrifuged at 4000g for 10 minutes, resuspended in anti-freeze solution and put in storage at -20°C.

Whole-brain clearing and staining

Lipophilic dye was applied to n=2 whole brains of *D. rerio*, *A. mexicanus*, *N. brichardi*, *C. anchorago* and *S. trutta* for fiber bundles tracing.

Brains stored in anti-freeze solution at -20°C were washed with PBST several times at room temperature (RT) for at least 1 day with gentle shaking. Samples were bleached for 2 hours under intense lighting (>10000 lux, GVL-SPOT-50-FIXV4-230VAC, GreenVisuaLED) in a fresh depigmentation solution of 5% H_2O_2, 0.05% sodium azide in PBS. The bleached samples were thoroughly washed with PBST at RT with rotation overnight. They were then subjected to a size-dependent delipidation step in CUBIC-L.[55] They were first immersed in a mixture of 50% PBST/50% CUBIC-L overnight at RT under gentle shaking followed by an incubation in CUBIC-L at 37°C under agitation for a variable duration (1-2 days for *D. rerio*, 3 days for *A. mexicanus*, 4 days for *N. brichardi* and 6 days for *C. anchorago* and *S. trutta* with solution renewed once). Delipidated specimens were washed with PBST for at least 4 hours at RT under gentle agitation (and eventually kept in PBST at 4°C for 1-5 additional days) prior to staining.

Staining was performed in solutions that were originally designed for immunostaining of zebrafish larvae [56]. Samples were immersed in a blocking solution of 10% (v/v) normal goat serum, 10% (v/v) DMSO, 5% (v/v) 1M PBS-glycine, 0.5% (v/v) Triton X-100, 0.1% (w/v) sodium deoxycholate, 0.1% (v/v) IGEPAL CA-630 and 0.1% (w/v) saponin in PBST overnight at 37°C under gentle shaking. Subsequently, specimens were stained with 2 µg/ml of DiI (D282, ThermoFisher Scientific) in a solution of 2% (v/v) NGS, 20% (v/v) DMSO, 0.05% (w/v) sodium azide, 0.2% (v/v) Triton-X100, 10 µg/mL heparin and 0.1% (w/v) saponin at 37°C under rotation for a specimen-dependent duration (2-3 days for *D. rerio*, 3 days for *A. mexicanus*, 4-5 days for *N. brichardi* and 6 days for *C. anchorago* and *S. trutta* with staining solution renewed

once). Some samples were also stained with a nuclear dye. In this case, following washes for at least 2 hours in PBST, they were labeled with YOYO-1 Iodide (Y3601, ThermoFisher Scientific, 1:250) in a solution of PBST supplemented with 500 mM NaCl at 37°C under agitation for the same duration than for DiI.

After a last washing step in PBST for a minimum of 2 hours at RT under shaking, refractive index (RI) matching was carried out in weakly basic CUBIC-R solution.[55] Brains were soaked in a mixture of 50% PBST/50% CUBIC-R overnight at RT under agitation and then kept in CUBIC-R (RI = 1.52) at RT for a few days or at 4°C for weeks prior to mounting.

Whole-brain mounting and 3D imaging

RI matched samples were embedded in a filtered (pore size 5.0 µm) melted agarose solution containing 2% (w/v) agarose, 70% (v/v) CUBIC-R in distilled H_2O. Once hardened, CUBIC/agarose gels were resectionned to adjust specimen orientation and immersed in CUBIC-R at RT for a minimum of 1 day to homogenize RIs.

Images were acquired with two commercial light-sheet fluorescence microscopes. Acquisitions were performed with an Ultramicroscope II (Miltenyi Biotec) using a 1.1x NA 0.1 MI PLAN objective and a DC57 WD17 0 dipping cap coupled to a 2x magnification lens, or a LVMI-Fluor 4x/0.3 WD6 objective without additional magnification. A Lightsheet 7 (Zeiss) equipped with 10x 0.2 foc illumination and 5x 0.16 foc detection optics was also used. In all cases, samples were glued (cyanoacrylate) to the dedicated sample holder and placed in the imaging cuvette filled with CUBIC-R (RI = 1.52). According to their size and the type of microscope images were acquired from dorsal or sagittal view. Cotton seed oil was poured on the surface of the imaging medium as an impermeable layer to avoid evaporation-induced RI changes during

imaging. 16-bit images were acquired by a pco.edge 5.5 sCMOS camera (2560 x 2160 pixels, pixel size 6.5 µm x 6.5 µm) on the Ultramicroscope II or a pco.edge 4.2 sCMOS camera (1920 × 1920 pixels, pixel size 6.5 µm × 6.5 µm) on the Lightsheet 7, following sample excitation with laser 488 and 561 nm. The z-step size was fixed to 6 µm on the Ultramicroscope II and 5.176 µm on the Lightsheet 7, which represents nearly half of the theoretical lightsheet thickness.

3D image reconstruction and manual segmentation

For the inter-species comparison of the anatomy of the tracts connecting the Tel with the rFM, these structures were segmented manually using the 3D visualization and reconstruction software Amira 2019 (Thermo Fisher Scientific).

The combination of the overall size of the specimens and the required resolution/voxel size demanded tiled image acquisition. The resulting image stacks were merged using the Grid/Collection stitching plugin[57] in fiji.[58]

In preparation for the manual segmentation, the signal-to-noise ratio of the merged data was improved by subtracting the gaussian noise (fiji, Gaussian Blur 3D, Kernel 10,10,10) from the original data. After manual segmentation of the original data and the denoised data, the defined regions were refined by multiplying the denoised data with the individual binary masks of the segmentations.

The 3D reconstructions in Figure 7 were produced on n=2 brains for each species by selective visualization of the denoised features under investigation in this study within the framework of the overall anatomy of the corresponding brains.

IL tract-tracing

In order to confirm the presence of the IL fiber tracts visualized with DiI staining, tract-tracing experiments were performed using NeuroVue (Polysciences), a lipophilic dye which allows both retrograde and anterograde tracing and can be used on fixed brain tissue.[59] Small triangular pieces of NeuroVue filter paper were inserted into the IL of n=3 specimens of *A. mexicanus*, *N. brichardi* and *C. anchorago*, and into the pallium of n=3 specimens of *N. brichardi*. Brains were then incubated at 36°C in 4% PFA in PBS for 4 (*A. mexicanus*) to 12 days (*C. anchorago*).

Following incubation, the NeuroVue filter paper was removed and brains were washed in PBS, then included in 3% agarose in H_2O. 80 µm sections were cut with a vibratome (Leica VT1200S) in the saggital plane for *A. mexicanus*, and for the *N. brichardi* specimens which were injected into the telencephalon. IL-injected *N. brichardi* and *C. anchorago* specimens were cut in the frontal plane. Sections were then treated with DAPI 1X in PBS for 20 min and washed in PBS before being mounted on glass slides with VectaShield mounting medium (Vector Laboratories). Sections were imaged using a Leica SP8 confocal microscope.

QUANTIFICATION AND STATISTICAL ANALYSIS

Cellular scaling rules of teleost brains

To determine whether brain mass, body mass, and total number of cells in the brain are correlated in teleosts, a nonparametric Spearman rank correlation test was used on log-transformed data. Previously published data on birds[10] and mammals [31] were used for comparison. If a $P<0.05$ value was found, reduced major axis (RMA) regressions were calculated using the SMATR package [60] in RStudio v.1.2.5033 and fitted RMA regression lines were added to the plots (Figure 2). To compare scaling among taxonomic groups, an analysis of covariance (ANCOVA) with post-hoc Sidak

corrected pairwise comparisons was used to check for significant differences in the slopes of the regression lines. In groups for which the slopes were statistically homogeneous, the regression lines were compared based on the differences in their intercepts.

Body mass and Brain mass, Total number of cells in the brain and Brain mass, and Body mass and Total number of cells in the brain were significantly correlated in all groups (Spearman r ranging from 0.945 to 1; $p<0.0001$ in all cases). Data on Columbiformes and Galliformes[10] was plotted as illustration but wasn't included in the statistical analysis due to the small sample size.

Regression lines for Body mass and Brain mass (Figure 2A) had significantly different slopes (ANCOVA, $p<0.0001$). Pairwise comparisons found significant differences in the slopes of Glires and Primates ($p<0.001$), Primates and Psittacopasserae ($p=0.0001$) and Primates and Teleosts ($p<0.0001$). ANCOVA revealed significant differences in the intercepts of the regression lines for Brain mass and Body mass for groups with statistically homogenous slopes ($p<0.0001$). Pairwise comparisons found significant differences in the intercepts of Glires, Teleosts and Psittacopasserae ($p<0.0001$ in all cases).

Regression lines for Body mass and Total number of cells in the brain (Figure 2B) had significantly different slopes (ANCOVA, $p<0.0001$). Pairwise comparisons found significant differences in the slopes of Glires and Primates ($p<0.001$), Primates and Psittacopasserae ($p<0.0001$) and Primates and Teleosts ($p<0.001$). ANCOVA revealed significant differences in the intercepts of the regression lines for Body mass and Total number of cells in the brain for groups with statistically homogenous slopes ($p<0.0001$). Pairwise comparisons found significant differences in the intercepts of Glires, Teleosts and Psittacopasserae ($p<0.05$ in all cases).

Regression lines for Total number of cells in the brain and Brain mass (Figure 2C) had significantly different slopes (ANCOVA, $p<0.0001$). Pairwise comparisons found significant differences in the slopes of Glires and Primates ($p<0.01$) and Primates and Psittacopasserae ($p<0.01$). ANCOVA revealed significant differences in the intercepts of the regression lines ($p<0.0001$). Pairwise comparisons found significant differences in the intercepts of the regression lines for Glires, Teleosts, Primates and Psittacopasserae ($p<0.0001$ in all cases), with the exception of the intercepts of Glires and Primates ($p=0.08$).

Degree of encephalization of sampled species

In order to determine the degree of encephalization of the teleost species sampled in this study, a phylogenetically corrected brain-body allometric slope was estimated using phylogenetically generalized least squares regression test (PGLS) at the Class level on species means of $\log^{10}$ brain and $\log^{10}$ body mass data of the species sampled in this study along with previously published actynopterygian data by Tsuboi et al. (2018)[7] using RStudio v.1.2.5033 with the CAPER package v.1.0.1 (Figure 3). Residual variance was modelled according to Brownian motion[61] and phylogenetic signal was estimated using Pagel's λ.[62] Phylogenetic relationships between teleost species were based on previously published phylogenetic trees.[63] The phylogenetic regression slope for actinopterygians was of 0.50 ± 0.01 (Adjusted R^2: 0.8382, $t=65.978$, $p<0.0001$).

Encephalization was then determined by extracting the residuals of $\log^{10}$-$\log^{10}$ brain and body mass for each species of the dataset to remove allometry in brain size.[64] The 11 species studied were ranked based on the value of their residual (Table S1).

Encephalization and relative mass and relative number of cells of major brain structures

To determine whether there exists a correlation between the degree of encephalization and relative mass and relative number of cells (expressed as the percentage of total brain mass and percentage of total brain cells, respectively) of the five major brain structures dissected, a nonparametric Spearman rank correlation test was used, as there was no way to ascertain the normal distribution of these data. We arranged species by decreasing order of encephalization (Figure S8). The test was performed in GraphPad Prism v.9.0.0 (GraphPad Software, San Diego, CA, USA) on species means. A significant negative correlation was found between encephalization and the relative mass and relative number of cells in the rH (Figure S8E, Spearman r: -0.7091, p=0.0268 and Spearman r: -0.6727, p=0.039, respectively). No significant correlation with encephalization was found in the four other brain structures for either relative mass or relative number of cells (Figures S8A-D, Tel relative mass: Spearman r: 0.4788, p=0.1663; relative number of cells: Spearman r: 0.01818, p=0.973; TeO relative mass: Spearman r: -0.1394, p=0.7072; relative number of cells: Spearman r: 0.1394, p=0.7072; rFM relative mass: Spearman r: 0.3333, p=0.3487; relative number of cells: Spearman r: -0.4788, p=0.1663; Cb relative mass: Spearman r: -0.1273, p=0.7330; relative number of cells: Spearman r: 0.4545, p=0.1912).

Species to species comparison of relative mass, absolute and relative number of cells in major brain structures

Normality of the data was tested using Shapiro-Wilk's test. As normality was not verified for all the species studied, and considering the small sample size, nonparametric Kruskal-Wallis and Dunn's post hoc tests were used to assess the inter-

species differences in relative mass, absolute and relative number of cells in the five dissected brain structures. All tests were performed in GraphPad Prism v. 9.0.0.

Significant differences were found in the absolute number of cells in all five structures (Kruskal-Wallis, $p<0.001$ in all cases). However, post-hoc pairwise comparisons revealed significant differences that were inconsistent across species and brain structures, the only consistently found difference across all structures being between *D. rerio* and *C. anchorago* (Dunn's test, $p<0.05$ in all cases).

Significant differences were found in the relative number of cells in all five structures (Kruskal-Wallis, $p<0.05$ in all cases). However, post-hoc pairwise comparisons revealed significant differences that were inconsistent across species and brain structures.

Significant differences were found in the relative mass in all five structures (Kruskal-Wallis, $p<0.05$ in all cases). However, post-hoc pairwise comparisons didn't reveal significant differences between species across the five structures, except for a modest difference in the relative mass of the rH between *A. mexicanus*, *C. anchorago* and *T. hardwicke* (Dunn's test, $p=0.0307$ and $p=0.0317$, respectively), and in the relative mass of the Tel between *C. anchorago* and *S. trutta* (Dunn's test, $p=0.0254$).

Comparison of relative mass and relative number of cells in major brain structures based on behavioral repertoire

Among the teleost species studied, wrasses display the most complex behavioral phenotypes. To determine whether this behavioral repertoire is associated with differences in relative mass and relative number of cells in major brain structures compared to other teleosts, the three species of wrasse (*C. anchorago* (n=4), *T. hardwicke* (n=3) and *L. dimidiatus* (n=3)) were grouped together (n=10) and compared

to all the other species (*M. zebra* (n=3), *N. brichardi* (n=5), *O. boops* (n=3), *A. nigrofasciata* (n=5), *A. mexicanus* (n=5), *D. rerio* (n=5) and *S. trutta* (n=4), grouped as "other fish" (n=30)) (Figures 5 and 6). As normality could not be satisfied for all structures in both groups, a nonparametric Mann-Whitney test was used. Regarding the relative mass, wrasses had a significantly larger Tel (Figure 5A) and rFM (Figure 5C) compared to other teleosts (Mann-Whitney's test, $p<0.0001$ and $p=0.0031$, respectively), and a significantly smaller Cb (Figure 5D) and rH (Figure 5E) ($p=0.0011$ and $p<0.0001$, respectively). No significant differences were found in the relative mass of the TeO (Figure 5B, $p=0.5483$). Regarding the relative number of cells, Wrasses had a significantly lower relative number of cells in the rH (Figure 6E) compared to the other teleosts (Mann-Whitney's test, $p<0.0001$). No significant differences were found in the relative number of cells of the other four structures (Figures 6A-D, Tel: $p=0.0538$; TeO: $p=0.3626$; rFM: $p=0.1983$; Cb: $p=0.8658$). Normality and Mann-Whitney tests were performed in GraphPad Prism v. 9.0.0.

Comparison of relative mass and relative number of cells in major brain structures based on phylogeny

In order to assess the differences in relative mass and relative number of cells in the five dissected brain structures based on phylogeny, species were grouped into different clusters: Cichlids and wrasses are part of the suborder Labrodei and are very closely phylogenetically related, and were thus grouped together as "Cichlids+Wrasses" (n=26). *A. mexicanus* (n=5) (Characidae), *D. rerio* (n=5) (Cyprinidae) and *S. trutta* (n=4) (Salmonidae) being phylogenetically distant, were grouped together as an "outgroup" (n=14) because of the n=1 species per family sample size.

We compared Cichlids+Wrasses to the "outgroup" using a nonparametric Mann-Whitney test, as normality could not be satisfied for all structures in both groups (Figures S10 and S11). Regarding the relative mass, Cichlids+Wrasses had a significantly larger Tel (Figure S10A) and rFM (Figure S10C) compared to the "outgroup" (Mann-Whitney's test, $p<0.0001$ in both structures), and a significantly smaller TeO (Figure S10B), Cb (Figure S10D) and rH (Figure S10E) ($p<0.0001$, $p=0.0211$ and $p<0.0001$, respectively). Regarding the relative number of cells, Cichlids+Wrasses had a significantly lower relative number of cells in the rH and a significantly higher relative number of cells in the rFM (Figure S11E) compared to the "outgroup" (Mann-Whitney's test, $p<0.0001$ and $p=0.0446$, respectively). No significant differences were found in the relative number of cells of the other three structures (Figure S11A, Tel: $p=0.1098$; Figure S11B, TeO: $p=0.3183$; Figure S11D, Cb: $p=0.6846$). All tests were performed in GraphPad Prism v. 9.0.0.

ACKNOWLEDGEMENTS

We thank Jean-Michel Hermel and Naomie Pradère (NeuroPSI, CNRS/Université Paris-Saclay) for their help with brain sampling. We thank Dimitri Rigaudeau (INRAE, Jouy-en-Josas) for providing us trouts and zebrafish, the DECA team (NeuroPSI) for *Astyanax* specimens, and Joël Attia (Université de Saint-Etienne) for cichlids, as well as the members of TEFOR animal facility (CNRS UMS2010, INRA UMS1451, Université Paris-Saclay), especially Krystel Saroul and Christophe de Medeiros for fish care. We thank members of NeuroPSI for technical support, and the MIMA2 platform (https://doi.org/10.15454/1.5572348210007727E12; INRAE, Jouy-en-Josas) for access to their lightsheet microscope.

AUTHOR CONTRIBUTIONS

Conceptualization, KY and PE; methodology, KY, PE, MS and AJ; funding acquisition and supervision, KY; validation and visualization, KY, PE, MS and AJ; first draft of manuscript, PE and KY.; all authors contributed to data analysis, interpretation, and revision of the manuscript.

DECLARATION OF INTERESTS

The authors declare no competing interests.

FIGURE TITLES AND LEGENDS

Figure 1. Phylogenetic tree of the teleost species sampled in this study. The families of wrasses and cichlids are the closest relatives within teleosts. In this study, we refer to the medaka, trout, *Astyanax*, and zebrafish as the "outgroup". Numbers at the root of each tree branches represent the estimated time of divergence (MYA: million years ago). The last common ancestor of these species can be traced back to 230 million years ago (http://www.timetree.org[50]).

Figure 2. Teleosts have small, cell-dense brains that contain more cells than the brains of rodents of similar body mass

The fitted reduced major axis (RMA) regression lines are displayed only for correlations that are significant. Each point represents the mean value of a species. X and y axes are in $\log^{10}$ scales. All regression lines are significantly different, except for the regression lines of Glires and Primates in plot (C).

(A) Brain mass plotted as a function of body mass. Teleosts have smaller brains than birds and mammals of similar body mass.

(B) Total number of cells in the brain plotted as a function of body mass. Teleost brains contain less cells than bird and primate brains, but more cells than the brains of rodents of similar body mass.

(C) Brain mass plotted as a function of total number of cells in the brain. Cellular density inside the teleost brain is higher than in birds and mammals.

Glires = rodents and lagomorphs. Psittacopasserae = Passeriformes (songbirds) and Psittaciformes (parrots).

See also Table 1. For statistics, see STAR Methods.

Figure 3. Encephalization in 11 species of teleosts (red) compared to a large dataset of actinopterygians (blue)

Brain mass is plotted as a function of body mass, and the phylogenetically corrected (phylogenetically generalized least squares regression test, PGLS) allometric line is shown. Each point represents the mean value of a species. X and y axes are in $\log^{10}$ scales. The phylogenetic regression slope for actinopterygians is of 0.50 ± 0.01. Adjusted R^2: 0.8382, t=65.978, p<0.0001.

See also Table S1 and STAR Methods.

Figure 4. Dissection of the five major brain structures of teleosts

(A) Lateral external view of the brain of the cichlid *Neolamprologus brichardi*. The different brain regions are color-coded. The uncolored regions are the olfactory bulbs and cranial nerves.

(B-E) 300 µm frontal sections of the brain of *Neolamprologus brichardi* from rostral to caudal, showing the boundaries of the five major brain regions. The regions are highlighted following the color code in (A).

Brain regions: Cb: cerebellum; Die: diencephalon; Hy: hypothalamus; IL: inferior lobe; ORRd: dorsal optic recess region; rFM: rest of the forebrain/midbrain; rH: rest of the hindrain; Tel: telencephalon; Tg: tegmentum; TeO: optic tectum; TS: torus semicircularis.

Scale bar: 1 mm.

R: rostral; C: caudal; D: dorsal; V: ventral.

See also STAR Methods.

Figure 5. Relatively larger Tel and rFM in wrasses compared to other teleosts

(A-E) Comparison of the relative mass of the Tel (A), TeO (B), rFM (C), Cb (D), and rH (E) of three species of wrasses (« Wrasses »: *Choerodon anchorago*, *Labroides dimidiatus*, *Thalassoma hardwicke*) and seven species of teleosts of various orders (« Other fish »: *Astyanax* mexicanus, *Amatitlania nigrofasciata, Danio rerio, Maylandia zebra, Neolamprologus brichardi, Ophtalmotilapia boops, Salmo* trutta). Wrasses have a relatively larger Tel and rFM compared to other teleosts. Statistical analysis: Mann-Whitney's test. Each point represents individual values.

ns: non significant, **p<0.01, ****p<0.0001.

Brain regions: Cb: cerebellum, rFM: rest of the forebrain/midbrain; rH: rest of the hindrain; Tel: telencephalon; TeO: optic tectum.

See also STAR Methods.

Figure 6. No increase in the relative number of cells in the Tel and rFM of wrasses compared to other teleosts

(A-E) Comparison of the relative number of cells in the Tel (A), TeO (B), rFM (C), Cb (D), and rH (E) of three species of wrasses (« Wrasses »: *Choerodon anchorago*,

Labroides dimidiatus, *Thalassoma hardwicke*) and seven species of teleosts of various orders (« Other fish »: *Astyanax* mexicanus, *Amatitlania nigrofasciata, Danio rerio, Maylandia zebra, Neolamprologus brichardi, Ophtalmotilapia boops, Salmo* trutta). Despite having a relatively larger Tel and rFM, wrasses don't have a larger proportion of cells in those structures compared to other teleosts. Statistical analysis: Mann-Whitney's test. Each point represents individual values.

ns: non significant, ****p<0.0001.

Brain regions: Cb: cerebellum, rFM: rest of the forebrain/midbrain; rH: rest of the hindrain; Tel: telencephalon; TeO: optic tectum.

See also STAR Methods.

Figure 7. The pallio-lobar tracts are massively enlarged in the wrasse and cichlid, while they are absent in the trout, the *Astyanax* surface fish and the zebrafish.

3D selective visualization of IL fiber tracts comparing the wrasse (*C. anchorago*; A), the cichlid (*N. brichardi*; B), the trout (*S. trutta*; C), the *Astyanax* surface fish (*A. mexicanus*; D), and the zebrafish (*D.* rerio; E). Lateral views are shown in A-E, while a dorsal view of one side of the wrasse brain is shown in F. Homologous tracts are shown in the same color across species. Besides wrasses and cichlids, no fibers connecting the pallium to the IL were found in the other species of teleosts examined, irrespective of brain size. The main connections of the IL in these species are with the PT (magenta), whereas they are with the pallium in wrasses and cichlids (Pal-IL tract in green, Pal-GR tract in magenta). Local IL networks are shown in purple, and PG projections to the pallium are shown in orange.

Brain regions : GR : corpus glomerulosum pars rotunda, IL: inferior lobe, PT: pretectum

R: rostral; C: caudal; D: dorsal; V: ventral; L: lateral ; M: medial.

Figure 8. Comparison of functional connectivity in relation to sensory inputs and motor outputs in amniotes and teleosts.

(A) Simplified diagram showing input/output connectivity of the pallium commonly found in mammals and birds (analogous, not necessarily homologous). Sensory inputs are shown in red, while motor outputs are shown in blue. The primary sensory areas in the pallium receive modal-specific sensory inputs from subtelencephalic sensory nuclei, mainly through the thalamus in the case of tetrapods. Note that there are two major visual pathways terminating in the pallium both in mammals and birds. The diagram is modified from Yamamoto and Bloch (2017).[51]

(B) Simplified diagram showing input/output connectivity of the pallium and IL in teleosts. The sensory afferents to the pallium in teleosts are mainly mediated via the PG instead of the thalamus. In addition to the pallium, IL receives sensory inputs of different modalities, here showing only visual and gustatory, which are the dominant ones. The pallium and IL are highly connected in some teleost groups such as wrasses and cichlids, but these connections are not detectable in other teleosts like zebrafish.

Sensory modalites: A: auditory, G: gustatory, S: somatosensory, Vte: visual (tectofugal), Vth: visual (thalamofugal).

Figure S1. Teleosts have small, cell-dense brains that contain more cells than the brains of rodents of similar body mass even after removal of the large *Choerodon anchorago* individual from the analysis.

The fitted reduced major axis (RMA) regression lines are displayed only for correlations that are significant. Each point represents the mean value of a species. X and y axes are in $\log^{10}$

scales. All regression lines are significantly different, except for the regression lines of Glires and Primates in plot (C).

(A) Brain mass plotted as a function of body mass. Teleosts have smaller brains than birds and mammals of similar body mass.

(B) Total number of cells in the brain plotted as a function of body mass. Teleost brains contain less cells than bird and primate brains, but more cells than the brains of rodents of similar body mass.

(C) Brain mass plotted as a function of total number of cells in the brain. Cellular density inside the teleost brain is higher than in birds and mammals.

Glires = rodents and lagomorphs. Psittacopasserae = Passeriformes (songbirds) and Psittaciformes (parrots).

See also Table S2. For statistics, see Document S1.

Figure S2. Encephalization in 11 species of teleosts compared to a large dataset of actinopterygians after removal of the large *Choerodon anchorago* individual.

Brain mass is plotted as a function of body mass, and the phylogenetically corrected (phylogenetically generalized least squares regression test, PGLS) allometric line is shown. Each point represents the mean value of a species. X and y axes are in $\log^{10}$ scales. The phylogenetic regression slope for actinopterygians is of 0.50 ± 0.01. Adjusted R^2: 0.8379, t=65.891, p<0.0001.

See also Table S3 and Document S1.

Figure S3. Encephalization in teleosts is not correlated with an increase in the relative mass or relative number of cells in the telencephalon even after removal of the large *Choerodon anchorago* individual from the analysis.

(A-E) Relative mass (triangles) and relative number of cells (open circles) of the Tel (A), TeO (B), rFM (C), Cb (D), and rH (E) of ten species of teleosts. Species are ranked from most encephalized (left) to least encephalized (right). Each point represents the mean value of a

species. Error bars show SD. Spearman's rank correlation test was used. Relative mass and relative number of cells in the rH (E) are negatively correlated with encephalization (Spearman r: -0.697, p=0.031 and Spearman r: -0.661, p=0.044), whereas no significant correlation exists for the other regions.

Species: Am: *Astyanax* mexicanus; An: *Amatitlania nigrofasciata*; Ca: *Choerodon anchorago*; Dr: *Danio rerio*; Ld: *Labroides dimidiatus*; Mz: *Maylandia zebra*; Nb: *Neolamprologus brichardi*; Ob: *Ophtalmotilapia boops*; St: *Salmo* trutta; Th: *Thalassoma hardwicke*;

Brain regions: Cb: cerebellum, rFM: rest of the forebrain/midbrain; rH: rest of the hindrain; Tel: telencephalon; TeO: optic tectum.

See also Document S1.

Figure S4. Relatively larger telencephalon (Tel) and rest of the forebrain/midbrain (rFM) in wrasses compared to other teleosts after removal of the large *Choerodon anchorago* individual from the analysis.

(A-E) Comparison of the relative mass of the Tel (A), TeO (B), rFM (C), Cb (D), and rH (E) of three species of wrasses (« Wrasses »: *Choerodon anchorago*, *Labroides dimidiatus*, *Thalassoma hardwicke*) and seven species of teleosts of various orders (« Other fish »: *Astyanax* mexicanus, *Amatitlania nigrofasciata, Danio rerio, Maylandia zebra, Neolamprologus brichardi, Ophtalmotilapia boops, Salmo* trutta). Wrasses have a relatively larger Tel and rFM compared to other teleosts. Statistical analysis: Mann-Whitney's test. Each point represents individual values.

ns: non significant, **p<0.01, ****p<0.0001.

Brain regions: Cb: cerebellum, rFM: rest of the forebrain/midbrain; rH: rest of the hindrain; Tel: telencephalon; TeO: optic tectum.

See also Document S1.

Figure S5. No increase in the relative number of cells in the telencephalon (Tel) and rest of the forebrain/midbrain (rFM) of wrasses compared to other teleosts after removal of the large *Choerodon anchorago* individual from the analysis.

(A-E) Comparison of the relative number of cells in the Tel (A), TeO (B), rFM (C), Cb (D), and rH (E) of three species of wrasses (« Wrasses »: *Choerodon anchorago*, *Labroides dimidiatus*, *Thalassoma hardwicke*) and seven species of teleosts of various orders (« Other fish »: *Astyanax* mexicanus, *Amatitlania nigrofasciata, Danio rerio, Maylandia zebra, Neolamprologus brichardi, Ophtalmotilapia boops, Salmo* trutta). Despite having a relatively larger Tel and rFM, wrasses don't have a larger proportion of cells in those structures compared to other teleosts. Statistical analysis: Mann-Whitney's test. Each point represents individual values.

ns: non significant, ****p<0.0001.

Brain regions: Cb: cerebellum, rFM: rest of the forebrain/midbrain; rH: rest of the hindrain; Tel: telencephalon; TeO: optic tectum.

See also Document S1.

Figure S6. Wrasses and cichlids have a relatively larger telencephalon (Tel) and rest of the forebrain/midbrain (rFM) compared to other teleosts even after removal of the large *Choerodon anchorago* individual from the analysis.

(A-E) Comparison of the relative mass of the Tel (A), TeO (B), rFM (C), Cb (D), and rH (E) of four species of cichlids and three species of wrasses (« Cichlids+Wrasses »: *Choerodon anchorago*, *Labroides dimidiatus*, *Thalassoma hardwicke, Amatitlania nigrofasciata, Maylandia zebra, Neolamprologus brichardi, Ophtalmotilapia boops*) and three species of teleosts of various orders (« Outgroup »: *Astyanax* mexicanus, *Danio rerio, Salmo* trutta). Cichlids+Wrasses have a relatively larger Tel and rFM compared to the outgroup. Statistical analysis: Mann-Whitney's test. Each point represents individual values.

*p<0.05, ****p<0.0001.

Brain regions: Cb: cerebellum, rFM: rest of the forebrain/midbrain; rH: rest of the hindrain; Tel: telencephalon; TeO: optic tectum.

See also Document S1.

Figure S7. Wrasses and cichlids have a similar relative number of cells in the telencephalon (Tel) and rest of the forebrain/midbrain (rFM) compared to other teleosts after removal of the large *Choerodon anchorago* individual from the analysis.

(A-E) Comparison of the relative number of cells in the Tel (A), TeO (B), rFM (C), Cb (D), and rH (E) of four species of cichlids and three species of wrasses (« Cichlids + Wrasses »: *Choerodon anchorago*, *Labroides dimidiatus*, *Thalassoma hardwicke, Amatitlania nigrofasciata, Maylandia zebra, Neolamprologus brichardi, Ophtalmotilapia boops*) and three species of teleosts of various orders (« Outgroup »: *Astyanax* mexicanus, *Danio rerio, Salmo* trutta). Cichlids+wrasses don't have a larger proportion of cells in the Tel nor in the rFM compared to the outgroup. Statistical analysis: Mann-Whitney's test. Each point represents individual values.

ns: non significant, ****p<0.0001.

Brain regions: Cb: cerebellum, rFM: rest of the forebrain/midbrain; rH: rest of the hindrain; Tel: telencephalon; TeO: optic tectum.

See also Document S1.

Figure S8. Encephalization in teleosts is not correlated with an increase in the relative mass or relative number of cells in the telencephalon (Tel)

(A-E) Relative mass (triangles) and relative number of cells (open circles) of the Tel (A), TeO (B), rFM (C), Cb (D), and rH (E) of ten species of teleosts. Species are ranked from most encephalized (left) to least encephalized (right). Each point represents the mean value of a species. Error bars show SD. Spearman's rank correlation test was used. Relative mass and relative number of cells in the rH (E) are negatively correlated with encephalization (Spearman

r: -0.709, p=0.027 and Spearman r: -0.673, p=0.039), whereas no significant correlation exists for the other regions.

Species: Am: *Astyanax* mexicanus; An: *Amatitlania nigrofasciata*; Ca: *Choerodon anchorago*; Dr: *Danio rerio*; Ld: *Labroides dimidiatus*; Mz: *Maylandia zebra*; Nb: *Neolamprologus brichardi*; Ob: *Ophtalmotilapia boops*; St: *Salmo* trutta; Th: *Thalassoma hardwicke*;

Brain regions: Cb: cerebellum, rFM: rest of the forebrain/midbrain; rH: rest of the hindrain; Tel: telencephalon; TeO: optic tectum.

See also STAR Methods.

Figure S9. Comparison of relative mass and number of cells in the brains of teleosts

Mass distribution and cellular composition of teleost brains appear to be similar across phylogeny when species are compared one to one. Relative mass (A) and number of cells (B) of the Tel, TeO, rFM, Cb and rH of ten teleost species. Values are mean percentages per species.

Species from left to right: “outgroup” (*Danio rerio*, *Astyanax mexicanus*, *Salmo trutta*), Cichlids (*Neolamprologus brichardi*, *Maylandia zebra*, *Amatitlania nigrofasciata*, *Ophthalmotilapia boops*), Wrasses (*Labroides dimidiatus*, *Thalassoma hardwicke*, *Choerodon anchorago)*.

Brain regions: Cb: cerebellum, rFM: rest of the forebrain/midbrain; rH: rest of the hindrain; Tel: telencephalon; TeO: optic tectum.

See also STAR Methods.

Figure S10. Wrasses and cichlids have a relatively larger telencephalon (Tel) and rest of the forebrain/midbrain (rFM) compared to other teleosts.

(A-E) Comparison of the relative mass of the Tel (A), TeO (B), rFM (C), Cb (D), and rH (E) of four species of cichlids and three species of wrasses (« Cichlids+Wrasses »: *Choerodon anchorago*, *Labroides dimidiatus*, *Thalassoma hardwicke, Amatitlania nigrofasciata, Maylandia zebra, Neolamprologus brichardi, Ophtalmotilapia boops*) and three species of teleosts of various orders (« Outgroup »: *Astyanax* mexicanus, *Danio rerio, Salmo* trutta).

Cichlids+Wrasses have a relatively larger Tel and rFM compared to the outgroup. Statistical analysis: Mann-Whitney's test. Each point represents individual values.

*p<0.05, ****p<0.0001.

Brain regions: Cb: cerebellum, rFM: rest of the forebrain/midbrain; rH: rest of the hindrain; Tel: telencephalon; TeO: optic tectum.

See also STAR Methods.

Figure S11. Wrasses and cichlids have a similar relative number of cells in the telencephalon (Tel) and a higher relative number of cells in the rest of the forebrain/midbrain (rFM) compared to other teleosts.

(A-E) Comparison of the relative number of cells in the Tel (A), TeO (B), rFM (C), Cb (D), and rH (E) of four species of cichlids and three species of wrasses (« Cichlids + Wrasses »: *Choerodon anchorago*, *Labroides dimidiatus*, *Thalassoma hardwicke, Amatitlania nigrofasciata, Maylandia zebra, Neolamprologus brichardi, Ophtalmotilapia boops*) and three species of teleosts of various orders (« Outgroup »: *Astyanax* mexicanus, *Danio rerio, Salmo* trutta). Cichlids+wrasses don't have a larger proportion of cells in the Tel, but a larger proportion in the rFM compared to the outgroup. Statistical analysis: Mann-Whitney's test. Each point represents individual values.

ns: non significant, *p<0.05, ****p<0.0001.

Brain regions: Cb: cerebellum, rFM: rest of the forebrain/midbrain; rH: rest of the hindrain; Tel: telencephalon; TeO: optic tectum.

See also STAR Methods.

Figure S12. Connectivity of the inferior lobe in the *Astyanax* surface fish and the cichlid.

Confocal images of DAPI-stained brain sections following NeuroVue injections in the IL of the *Astyanax* surface fish (*A. mexicanus*; A) and the cichlid (*N. brichardi*; B), and in the pallium of *N. brichardi* (C, D).

(A) Sagittal section of the *Astyanax* midbrain. Fibers and terminals are visible in the ipsilateral PT, indicating the presence of ascending projections from IL.

(B) Frontal section of a cichlid brain injected with NeuroVue in the IL at the level of the TeO. Like in the *Astyanax*, fibers and terminals (in magenta) are visible in the ipsilateral PT, indicating the presence of ascending projections from the IL.

(C, D) Sagittal sections of a cichlid brain. The rostral half of the telencephalon was cut in the frontal plane to allow for precise NeuroVue injection. Following NeuroVue injections in the pallium, fibers and terminals (in magenta) were visible in the ipsilateral GR (C) and IL (D), indicating the presence of descending projections from the pallium to the IL through the Pal-GR and Pal-IL tracts, respectively.

Brain regions: GR: corpus glomerulosum pars rotunda, IL: inferior lobe, PT: pretectum

R: rostral; C: caudal; D: dorsal; V: ventral; L: lateral; M: medial.

REFERENCES

1. Emery, N.J., and Clayton, N.S. (2004). The mentality of crows: convergent evolution of intelligence in corvids and apes. Science (New York, N.Y *306*, 1903–1907.

2. Kirsch, J.A., Gunturkun, O., and Rose, J. (2008). Insight without cortex: lessons from the avian brain. Consciousness and cognition *17*, 475–483.

3. Hunt, G.R. (1996). Manufacture and use of hook-tools by New Caledonian crows. Nature *379*, 249–251. 10.1038/379249a0.

4. Hunt, G.R., and Gray, R.D. (2004). The crafting of hook tools by wild New Caledonian crows. Proc Biol Sci *271*, S88–S90.

5. Auersperg, A.M.I., Szabo, B., von Bayern, A.M.P., and Kacelnik, A. (2012). Spontaneous innovation in tool manufacture and use in a Goffin's cockatoo. Curr. Biol. *22*, R903-904. 10.1016/j.cub.2012.09.002.

6. Prior, H., Schwarz, A., and Güntürkün, O. (2008). Mirror-induced behavior in the magpie (Pica pica): evidence of self-recognition. PLoS Biol. *6*, e202. 10.1371/journal.pbio.0060202.

7. Tsuboi, M., van der Bijl, W., Kopperud, B.T., Erritzøe, J., Voje, K.L., Kotrschal, A., Yopak, K.E., Collin, S.P., Iwaniuk, A.N., and Kolm, N. (2018). Breakdown of brain-body allometry and the encephalization of birds and mammals. Nat Ecol Evol *2*, 1492–1500. 10.1038/s41559-018-0632-1.

8. MacLean, E.L., Hare, B., Nunn, C.L., Addessi, E., Amici, F., Anderson, R.C., Aureli, F., Baker, J.M., Bania, A.E., Barnard, A.M., et al. (2014). The evolution of self-control. Proc Natl Acad Sci U S A *111*, E2140-2148. 10.1073/pnas.1323533111.

9. Benson-Amram, S., Dantzer, B., Stricker, G., Swanson, E.M., and Holekamp, K.E. (2016). Brain size predicts problem-solving ability in mammalian carnivores. Proc Natl Acad Sci U S A *113*, 2532–2537. 10.1073/pnas.1505913113.

10. Olkowicz, S., Kocourek, M., Lučan, R.K., Porteš, M., Fitch, W.T., Herculano-Houzel, S., and Němec, P. (2016). Birds have primate-like numbers of neurons in the forebrain. Proc. Natl. Acad. Sci. U.S.A. *113*, 7255–7260. 10.1073/pnas.1517131113.

11. Brown, C. (2012). Tool use in fishes. Fish and Fisheries *13*, 105–115.

12. Kohda, M., Hotta, T., Takeyama, T., Awata, S., Tanaka, H., Asai, J.-Y., and Jordan, A.L. (2019). If a fish can pass the mark test, what are the implications for consciousness and self-awareness testing in animals? PLoS Biol. *17*, e3000021. 10.1371/journal.pbio.3000021.

13. Bloch, S., Thomas, M., Colin, I., Galant, S., Machado, E., Affaticati, P., Jenett, A., and Yamamoto, K. (2019). Mesencephalic origin of the inferior lobe in zebrafish. BMC Biol. *17*, 22. 10.1186/s12915-019-0631-y.

14. Bloch, S., Froc, C., Pontiggia, A., and Yamamoto, K. (2019). Existence of working memory in teleosts: Establishment of the delayed matching-to-sample task in adult zebrafish. Behav. Brain Res. *370*, 111924. 10.1016/j.bbr.2019.111924.

15. Bloch, S., Hagio, H., Thomas, M., Heuzé, A., Hermel, J.-M., Lasserre, E., Colin, I., Saka, K., Affaticati, P., Jenett, A., et al. (2020). Non-thalamic origin of zebrafish sensory nuclei implies convergent evolution of visual pathways in amniotes and teleosts. eLife *9*. 10.7554/eLife.54945.

16. Yamamoto, K., Bloch, S., and Vernier, P. (2017). New perspective on the regionalization of the anterior forebrain in Osteichthyes. Dev. Growth Differ. *59*, 175–187. 10.1111/dgd.12348.

17. Bernardi, G. (2012). The use of tools by wrasses (Labridae). Coral Reefs *31*, 39–39. 10.1007/s00338-011-0823-6.

18. Paśko, Ł. (2010). Tool-like behavior in the sixbar wrasse, Thalassoma hardwicke (Bennett, 1830). Zoo Biol *29*, 767–773. 10.1002/zoo.20307.

19. Kohda, M., Sogawa, S., Jordan, A.L., Kubo, N., Awata, S., Satoh, S., Kobayashi, T., Fujita, A., and Bshary, R. (2022). Further evidence for the capacity of mirror self-recognition in cleaner fish and the significance of ecologically relevant marks. PLoS Biol *20*, e3001529. 10.1371/journal.pbio.3001529.

20. McAuliffe, K., Drayton, L.A., Royka, A., Aellen, M., Santos, L.R., and Bshary, R. (2021). Cleaner fish are sensitive to what their partners can and cannot see. Commun Biol *4*, 1127. 10.1038/s42003-021-02584-2.

21. Wismer, S., Grutter, A., and Bshary, R. (2016). Generalized rule application in bluestreak cleaner wrasse (Labroides dimidiatus): using predator species as social tools to reduce punishment. Anim Cogn *19*, 769–778. 10.1007/s10071-016-0975-4.

22. Schluessel, V., Kreuter, N., Gosemann, I.M., and Schmidt, E. (2022). Cichlids and stingrays can add and subtract 'one' in the number space from one to five. Sci Rep *12*, 3894. 10.1038/s41598-022-07552-2.

23. Hotta, T., Kawasaka, K., Satoh, S., and Kohda, M. (2019). Fish focus primarily on the faces of other fish. Sci Rep *9*, 8377. 10.1038/s41598-019-44715-0.

24. Snekser, J.L., and Itzkowitz, M. (2020). Convict cichlid parents that stay with the same mate develop unique and consistent divisions of roles. PeerJ *8*, e10534. 10.7717/peerj.10534.

25. Barks, P.M., and Godin, J.-G.J. (2013). Can convict Cichlids (Amatitlania siquia) socially learn the degree of predation risk associated with novel visual cues in their environment? PLoS One *8*, e75858. 10.1371/journal.pone.0075858.

26. Sakamoto, N., and Ito, H. (1982). Fiber connections of the corpus glomerulosum in a teleost, Navodon modestus. J Comp Neurol *205*, 291–298. 10.1002/cne.902050309.

27. Yang, C.-Y., Xue, H.-G., Yoshimoto, M., Ito, H., Yamamoto, N., and Ozawa, H. (2007). Fiber connections of the corpus glomerulosum pars rotunda, with special reference to efferent projection pattern to the inferior lobe in a percomorph teleost, tilapia (Oreochromis niloticus). J. Comp. Neurol. *501*, 582–607. 10.1002/cne.21261.

28. Shimizu, M., Yamamoto, N., Yoshimoto, M., and Ito, H. (1999). Fiber connections of the inferior lobe in a percomorph teleost, Thamnaconus (Navodon) modestus. Brain Behav. Evol. *54*, 127–146. 10.1159/000006618.

29. Yamamoto, N., and Ito, H. (2008). Visual, lateral line, and auditory ascending pathways to the dorsal telencephalic area through the rostrolateral region of the lateral preglomerular nucleus in cyprinids. J. Comp. Neurol. *508*, 615–647. 10.1002/cne.21717.

30. Zhang, K., and Sejnowski, T.J. (2000). A universal scaling law between gray matter and white matter of cerebral cortex. Proc Natl Acad Sci U S A *97*, 5621–5626. 10.1073/pnas.090504197.

31. Herculano-Houzel, S., Catania, K., Manger, P.R., and Kaas, J.H. (2015). Mammalian Brains Are Made of These: A Dataset of the Numbers and Densities of Neuronal and Nonneuronal Cells in the Brain of Glires, Primates, Scandentia, Eulipotyphlans, Afrotherians and Artiodactyls, and Their Relationship with Body Mass. Brain, Behavior and Evolution *86*, 145–163. 10.1159/000437413.

32. Reiner, A., Medina, L., and Veenman, C.L. (1998). Structural and functional evolution of the basal ganglia in vertebrates. Brain research *28*, 235–285.

33. Albin, R.L., Young, A.B., and Penney, J.B. (1989). The functional anatomy of basal ganglia disorders. Trends Neurosci *12*, 366–375. 10.1016/0166-2236(89)90074-x.

34. Schmidt, M. (2020). Evolution of the Hypothalamus and Inferior Lobe in Ray-Finned Fishes. Brain Behav Evol *95*, 302–316. 10.1159/000505898.

35. Demski, L.S., and Knigge, K.M. (1971). The telencephalon and hypothalamus of the bluegill (Lepomis macrochirus): evoked feeding, aggressive and reproductive behavior with representative frontal sections. J. Comp. Neurol. *143*, 1–16. 10.1002/cne.901430102.

36. Demski, L.S. (1973). Feeding and aggressive behavior evoked by hypothalamic stimulation in a cichlid fish. Comp Biochem Physiol A Comp Physiol *44*, 685–692.

37. Muto, A., Lal, P., Ailani, D., Abe, G., Itoh, M., and Kawakami, K. (2017). Activation of the hypothalamic feeding centre upon visual prey detection. Nat Commun *8*, 15029. 10.1038/ncomms15029.

38. Roberts, M.G., and Savage, G.E. (1978). Effects of hypothalamic lesions on the food intake of the goldfish (Carassius auratus). Brain Behav. Evol. *15*, 150–164. 10.1159/000123777.

39. Morita, Y., Ito, H., and Masai, H. (1980). Central gustatory paths in the crucian carp, Carassius carassius. J. Comp. Neurol. *191*, 119–132. 10.1002/cne.901910107.

40. Rink, E., and Wullimann, M.F. (1998). Some forebrain connections of the gustatory system in the goldfish Carassius auratus visualized by separate DiI application to the hypothalamic inferior lobe and the torus lateralis. J. Comp. Neurol. *394*, 152–170.

41. Morita, Y., Murakami, T., and Ito, H. (1983). Cytoarchitecture and topographic projections of the gustatory centers in a teleost, Carassius carassius. J Comp Neurol *218*, 378–394. 10.1002/cne.902180403.

42. Ahrens, K., and Wullimann, M.F. (2002). Hypothalamic inferior lobe and lateral torus connections in a percomorph teleost, the red cichlid (Hemichromis lifalili). J. Comp. Neurol. *449*, 43–64. 10.1002/cne.10264.

43. Yang, C.-Y., Yoshimoto, M., Xue, H.-G., Yamamoto, N., Imura, K., Sawai, N., Ishikawa, Y., and Ito, H. (2004). Fiber connections of the lateral valvular nucleus in a percomorph teleost, tilapia (Oreochromis niloticus). J Comp Neurol *474*, 209–226. 10.1002/cne.20150.

44. Kubo, F., Hablitzel, B., Dal Maschio, M., Driever, W., Baier, H., and Arrenberg, A.B. (2014). Functional architecture of an optic flow-responsive area that drives horizontal eye movements in zebrafish. Neuron *81*, 1344–1359. 10.1016/j.neuron.2014.02.043.

45. Portugues, R., Feierstein, C.E., Engert, F., and Orger, M.B. (2014). Whole-brain activity maps reveal stereotyped, distributed networks for visuomotor behavior. Neuron *81*, 1328–1343. 10.1016/j.neuron.2014.01.019.

46. Fajardo, O., Zhu, P., and Friedrich, R.W. (2013). Control of a specific motor program by a small brain area in zebrafish. Front Neural Circuits *7*, 67. 10.3389/fncir.2013.00067.

47. Ströckens, F., Neves, K., Kirchem, S., Schwab, C., Herculano-Houzel, S., and Güntürkün, O. (2022). High associative neuron numbers could drive cognitive performance in corvid species. J Comp Neurol. 10.1002/cne.25298.

48. Fuster, J.M. (2002). Frontal lobe and cognitive development. J. Neurocytol. *31*, 373–385. 10.1023/a:1024190429920.

49. Izawa, E.-I., and Watanabe, S. (2008). Neuroanatomical and behavioural studies on dominance linearity in the crow. In CARLS Series of Advanced Study of Logic and Sensibility Vol. 2, S. Watanabe, ed. (Keio University Press), pp. 49–58.

50. Kumar, S., Suleski, M., Craig, J.M., Kasprowicz, A.E., Sanderford, M., Li, M., Stecher, G., and Hedges, S.B. (2022). TimeTree 5: An Expanded Resource for Species Divergence Times. Molecular Biology and Evolution *39*, msac174. 10.1093/molbev/msac174.

51. Yamamoto, K., and Bloch, S. (2017). Overview of Brain Evolution : Lobe-Finned Fish vs. Ray-Finned Fish. In Evolution of the Brain, Cognition, and Emotion in Vertebrates, S. Watanabe, M. A. Hofman, and T. Shimizu, eds. (Springer), pp. 3–33.

52. Herculano-Houzel, S., and Lent, R. (2005). Isotropic fractionator: a simple, rapid method for the quantification of total cell and neuron numbers in the brain. J. Neurosci. *25*, 2518–2521. 10.1523/JNEUROSCI.4526-04.2005.

53. Bahney, J., and von Bartheld, C.S. (2014). Validation of the isotropic fractionator: comparison with unbiased stereology and DNA extraction for quantification of glial cells. J Neurosci Methods *222*, 165–174. 10.1016/j.jneumeth.2013.11.002.

54. Miller, D.J., Balaram, P., Young, N.A., and Kaas, J.H. (2014). Three counting methods agree on cell and neuron number in chimpanzee primary visual cortex. Front Neuroanat *8*, 36. 10.3389/fnana.2014.00036.

55. Tainaka, K., Murakami, T.C., Susaki, E.A., Shimizu, C., Saito, R., Takahashi, K., Hayashi-Takagi, A., Sekiya, H., Arima, Y., Nojima, S., et al. (2018). Chemical Landscape for Tissue Clearing Based on Hydrophilic Reagents. Cell Rep *24*, 2196-2210.e9. 10.1016/j.celrep.2018.07.056.

56. Lempereur, S., Machado, E., Licata, F., Simion, M., Buzer, L., Robineau, I., Hémon, J., Banerjee, P., De Crozé, N., Léonard, M., et al. (2022). ZeBraInspector, a platform for the automated segmentation and analysis of body and brain volumes in whole 5 days post-fertilization zebrafish following simultaneous visualization with identical orientations. Developmental Biology *490*, 86–99. 10.1016/j.ydbio.2022.07.004.

57. Preibisch, S., Saalfeld, S., and Tomancak, P. (2009). Globally optimal stitching of tiled 3D microscopic image acquisitions. Bioinformatics *25*, 1463–1465. 10.1093/bioinformatics/btp184.

58. Schindelin, J., Arganda-Carreras, I., Frise, E., Kaynig, V., Longair, M., Pietzsch, T., Preibisch, S., Rueden, C., Saalfeld, S., Schmid, B., et al. (2012). Fiji: an open-source platform for biological-image analysis. Nature methods *9*, 676–682.

59. Duncan, J., Kersigo, J., Gray, B., and Fritzsch, B. (2011). Combining lipophilic dye, in situ hybridization, immunohistochemistry, and histology. J Vis Exp, 2451. 10.3791/2451.

60. Warton, D.I., Duursma, R.A., Falster, D.S., and Taskinen, S. (2012). smatr 3– an R package for estimation and inference about allometric lines. Methods in Ecology and Evolution *3*, 257–259. 10.1111/j.2041-210X.2011.00153.x.

61. Felsenstein, J. (1985). Phylogenies and the Comparative Method. The American Naturalist *125*, 1–15.

62. Lynch, M. (1991). METHODS FOR THE ANALYSIS OF COMPARATIVE DATA

IN EVOLUTIONARY BIOLOGY. Evolution *45*, 1065–1080. 10.1111/j.1558-5646.1991.tb04375.x.

63. Rabosky, D.L., Santini, F., Eastman, J., Smith, S.A., Sidlauskas, B., Chang, J., and Alfaro, M.E. (2013). Rates of speciation and morphological evolution are correlated across the largest vertebrate radiation. Nat Commun *4*, 1958. 10.1038/ncomms2958.

64. Sol, D., Sayol, F., Ducatez, S., and Lefebvre, L. (2016). The life-history basis of behavioural innovations. Philos Trans R Soc Lond B Biol Sci *371*, 20150187. 10.1098/rstb.2015.0187.

Table 1. Cellular composition of the brains of 11 teleost species. All values are mean ± SD.

Species	n	Body mass (g)	Brain mass (mg)	Total cells (x10^6)
Wrasses				
Labroides dimidiatus	3	1.55 ± 0.35	34.62 ± 5.62	45.7 ± 6.67
Thalassoma hardwicke	3	12.07 ± 4.14	132.82 ± 23.49	116.78 ± 25.62
Choerodon anchorago	4	91.52 ± 137.39	338.80 ± 206.95	185.08 ± 78.73
Cichlids				
Neolamprologus brichardi	5	5.15 ± 1.53	42.43 ± 4.26	37.54 ± 7.08
Amatitlania nigrofasciata	5	20.28 ± 7.85	75.05 ± 12.4	56.62 ± 6.37
Opthalmotilapia boops	3	7.04 ± 2.39	80.32 ± 7.27	56.37 ± 6.35
Maylandia zebra	3	14.59 ± 2.58	96.94 ± 6.62	61.78 ± 3.72
Others				
Oryzias latipes	5	0.492 ± 0.07	8.38 ± 1.12	6.66 ± 0.54
Danio rerio	5	0.73 ± 0.21	9.74 ± 0.2	8.92 ± 0.69
Astyanax mexicanus	5	3.7 ± 1.17	43.55 ± 4.35	26.09 ± 2.74
Salmo trutta	4	177.15 ± 45.05	354.73 ± 33.16	100.84 ± 8.58

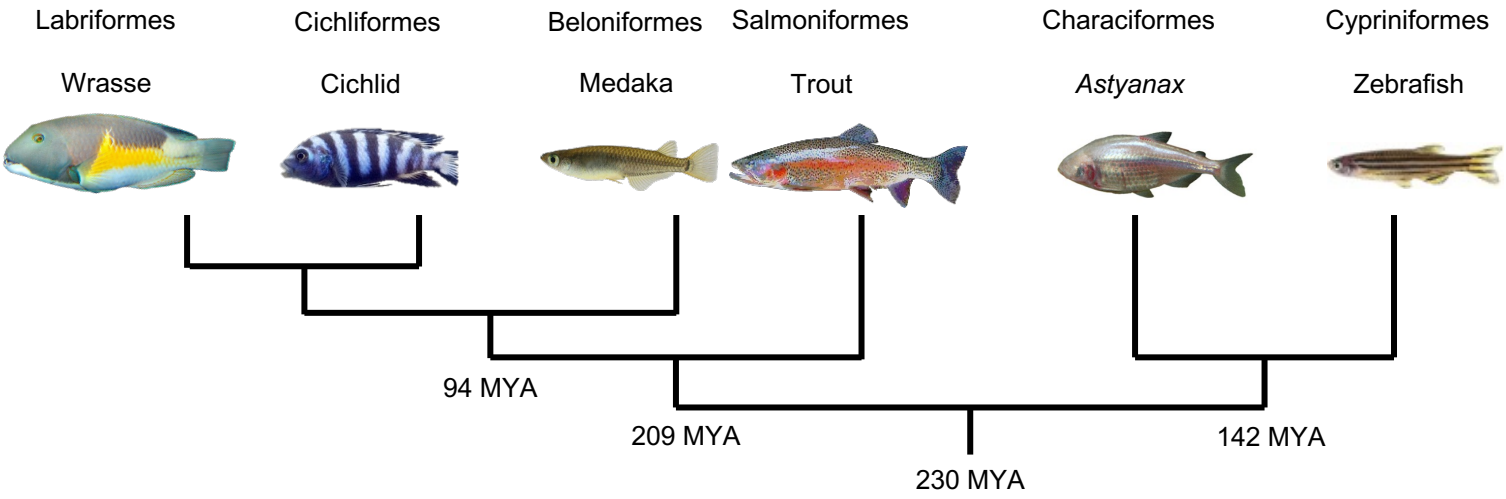

Figure 1.

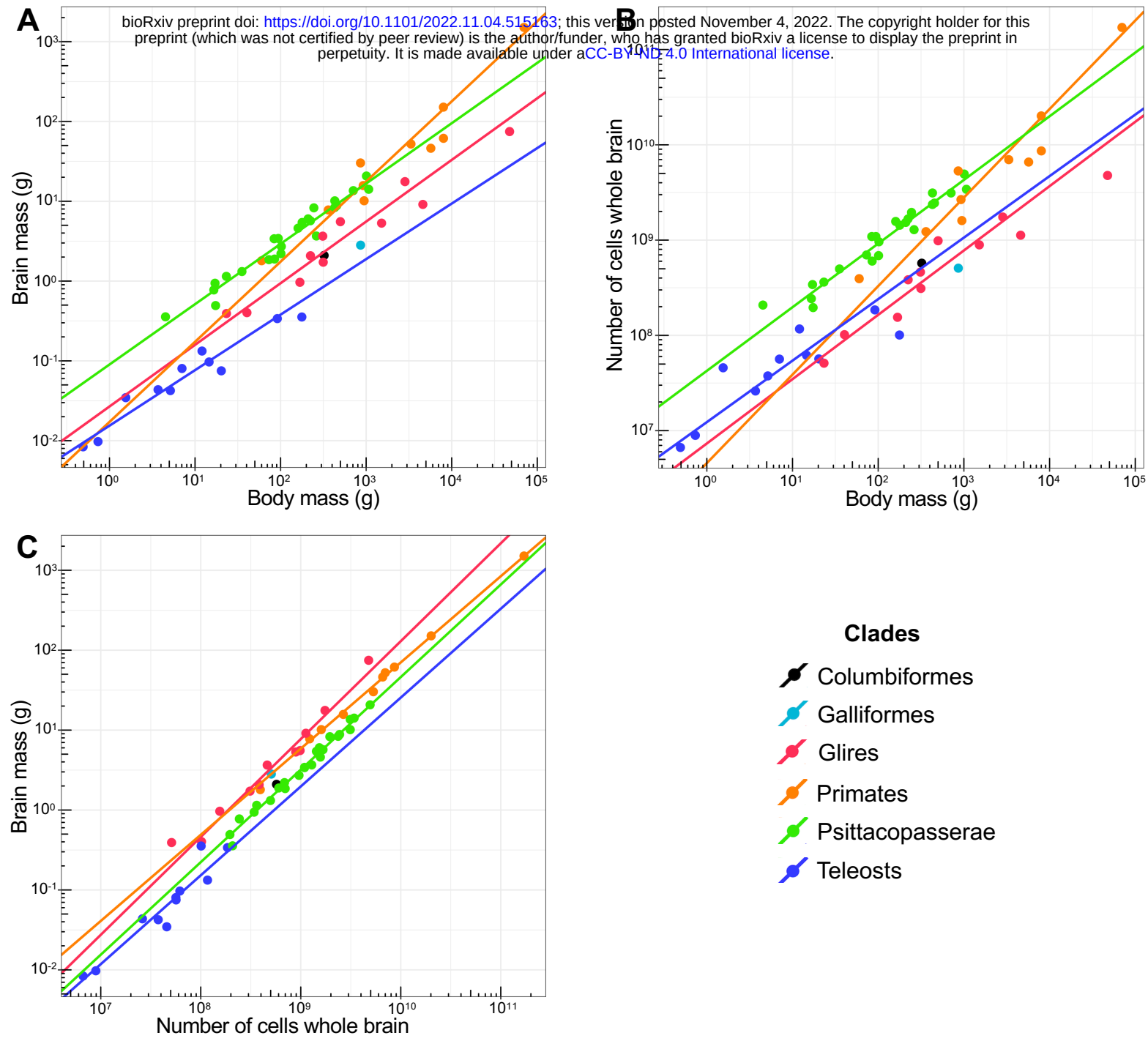

Figure 2.

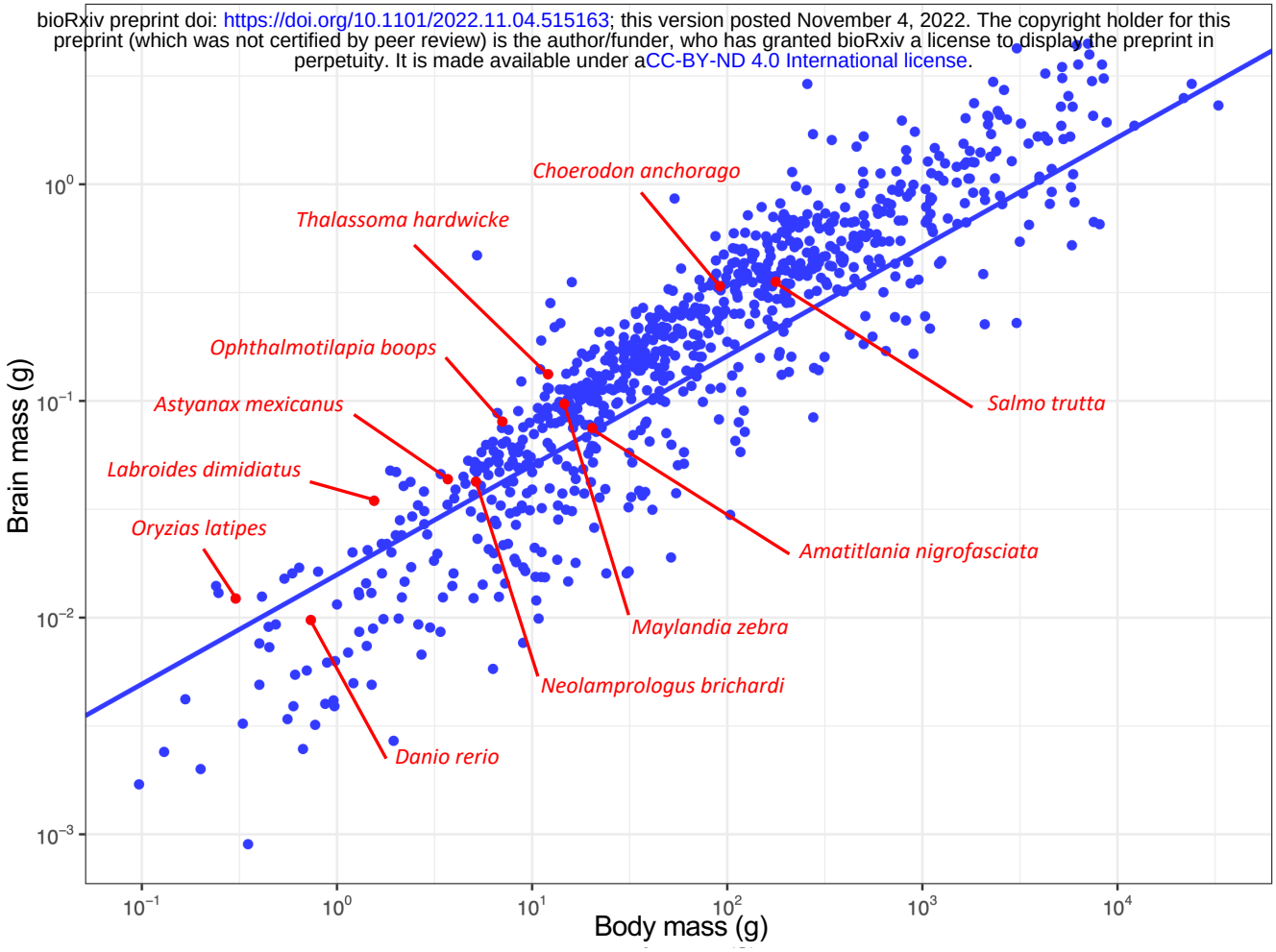

Figure 3.

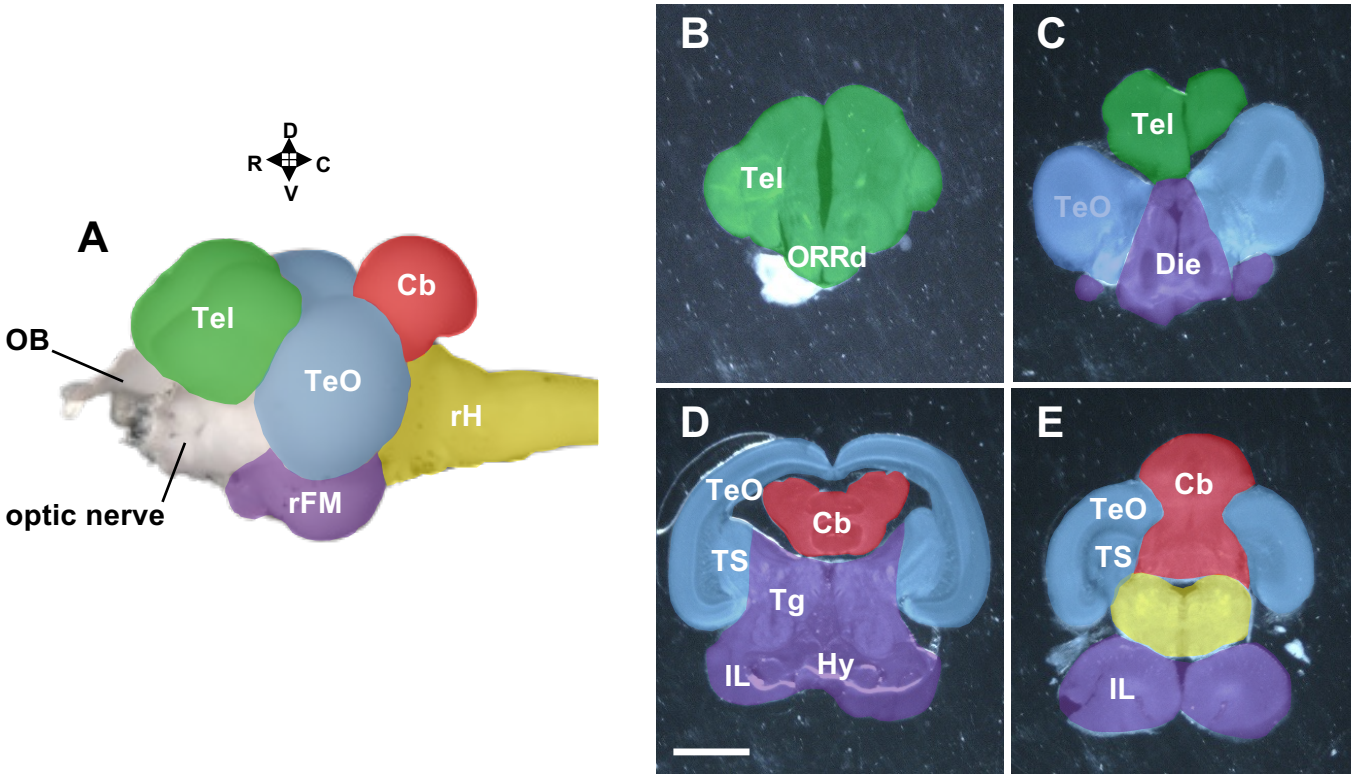

Figure 4.

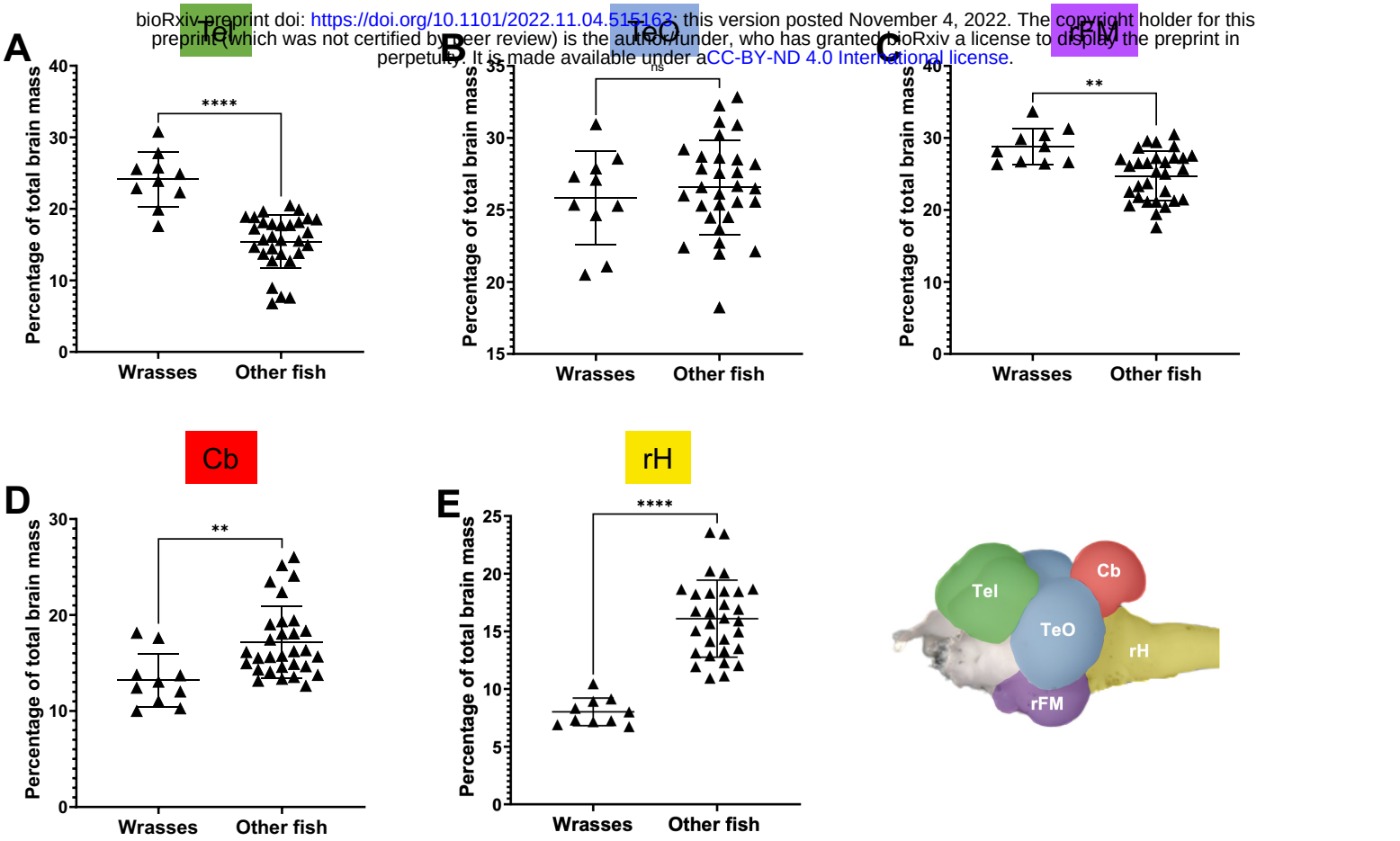

Figure 5.

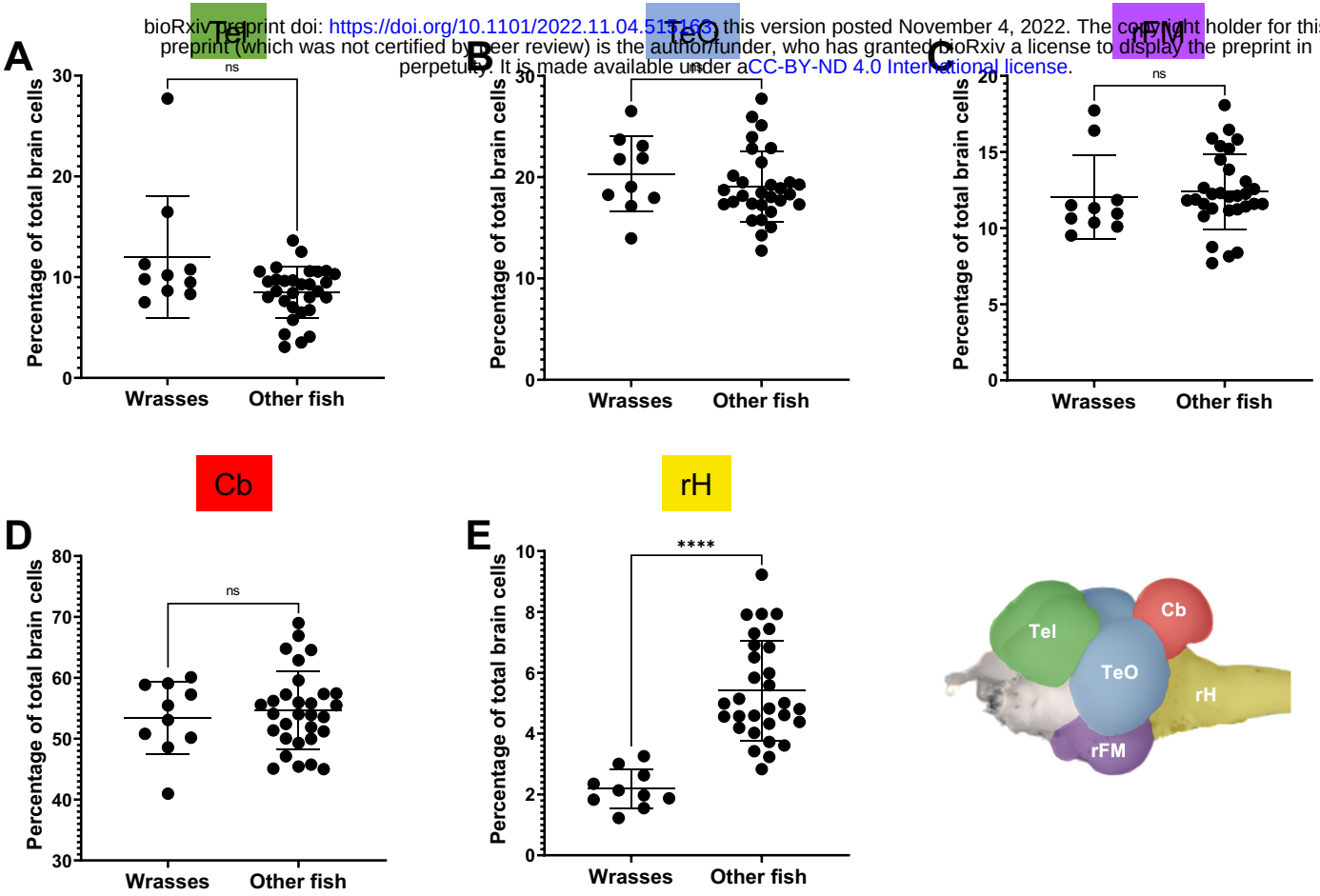

Figure 6.

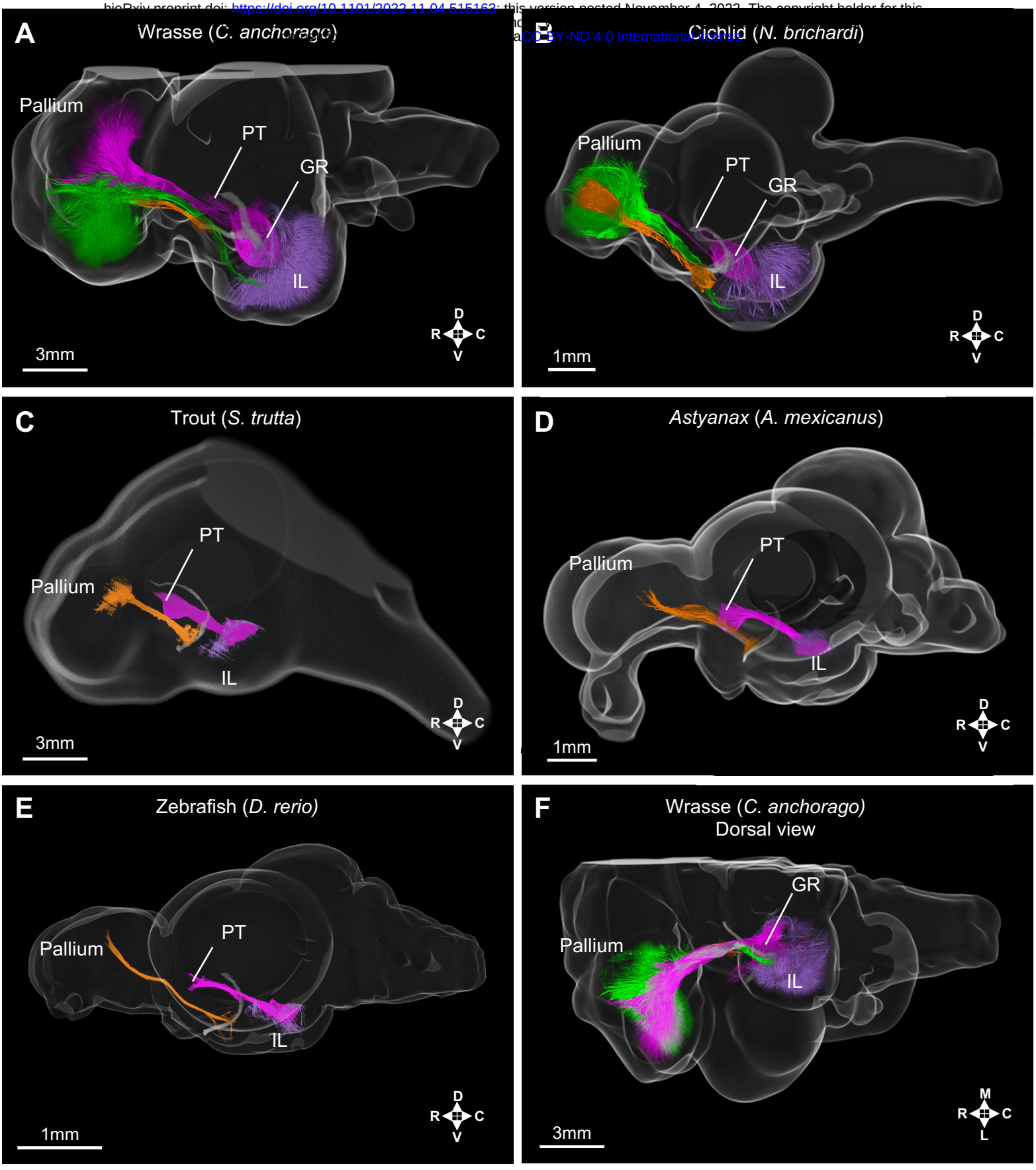

Figure 7.

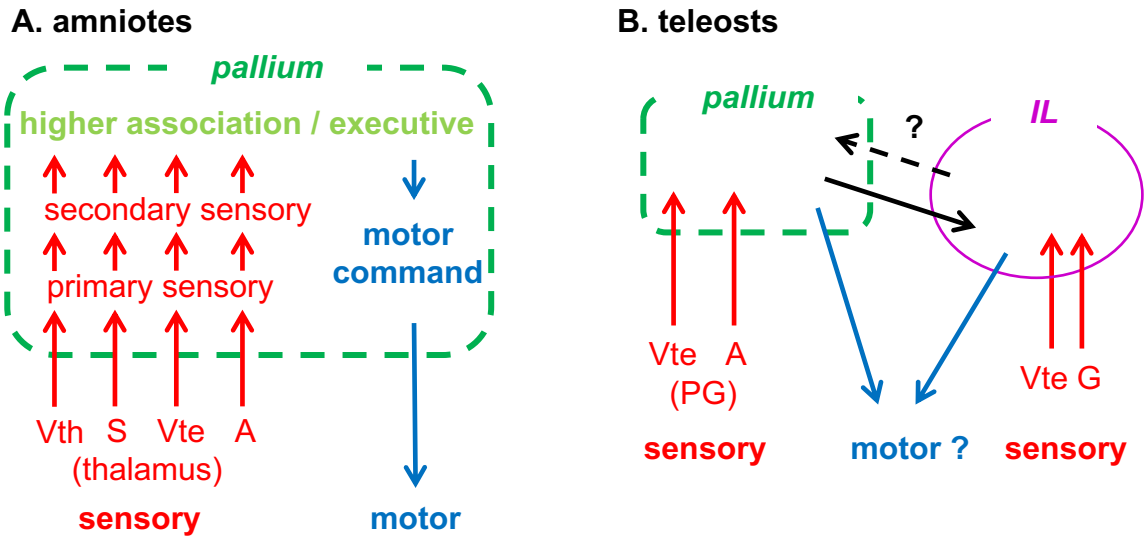
A. amniotes
pallium
higher association / executive
secondary sensory
primary sensory
motor command
Vth
S
Vte
A
(thalamus)
sensory
motor
B. teleosts
pallium
?
IL
Vte
A
(PG)
Vte G
sensory
motor ?
sensory

Figure 8.